THE STUDY OF COLLISION-INDUCED PHENOMENA WITH A DEMPSTER-TYPE MASS SPECTROMETER

THESIS FOR THE DEGREE OF Ph. D.
MICHIGAN STATE UNIVERSITY
HAROLD H. HARRIS
1967

This is to certify that the

thesis entitled

THE STUDY OF COLLISION-INDUCED PHENOMENA
WITH A DEMPSTER-TYPE MASS SPECTROMETER

presented by

Harold H. Harris

**has been accepted towards fulfillment
of the requirements for**

Ph. D. **degree in** Chemistry

Morley Russell
Major professor

Date January 7, 1967

O-169

ABSTRACT

THE STUDY OF COLLISION-INDUCED PHENOMENA WITH A DEMPSTER-TYPE MASS SPECTROMETER

by Harold H. Harris

In spite of the large number of Dempster-type analytical mass spectrometers in use, this instrument has not been used in the study of collision-induced phenomena. The reason for this is that there is only a small volume in the spectrometer in which reactions can occur and have the products appear in the mass spectrum. When the analyzer pressure is high enough so that a measurable number of reactions occur, it is also high enough to attenuate the ion beams. Whenever such attenuation exceeds a few percent, the equations usually used to calculate the reaction cross sections are not valid.

In the present work, new equations are developed for use in the measurement of both total collision cross sections and reaction cross sections in a Dempster mass spectrometer. Experimental studies are made of the following reactions, and their reaction cross sections are determined at 1000 volts ion accelerating potential:

(1) $Ar^{+2} + Ar \longrightarrow Ar^{+} + Ar^{+}$ $\sigma = 3.6 \times 10^{-16}$ cm^{2}

(2) $CO^{+} + CO_2 \longrightarrow C^{+} + O + CO_2$ $\sigma = 6.6 \times 10^{-17}$ cm^{2}

(3) $N_2^{+} + N_2 \longrightarrow N^{+} + N + N_2$ $\sigma = 3.5 \times 10^{-17}$ cm^{2}

(4) $N_2O^{+} + N_2O \longrightarrow NO^{+} + N + N_2O$ $\sigma = 6.3 \times 10^{-17}$ cm^{2}

(5) $CO^{+2} + CO \longrightarrow C^{+} + (O^{+}) + (CO^{+})$ $\sigma = 1.4 \times 10^{-17}$ cm^{2}

The value of Kuprianov and co-workers (1) of 1.0×10^{-17} cm^{2} for the reaction

(6) $CO^{+} + CO \longrightarrow C^{+} + O + CO$

was used for calibration.

In addition, the total collision cross sections for the following systems were determined:

CO^{+} in CO $\sigma_T = 2.4 \times 10^{-16}$ cm^{2}

O^{+} in CO $\sigma_T = 5.0 \times 10^{-17}$ cm^{2}

C^{+} in CO $\sigma_T = 1.8 \times 10^{-16}$ cm^{2}

Ar^{+} in Ar $\sigma_T = 2.2 \times 10^{-15}$ cm^{2}

Ar^{+2} in Ar $\sigma_T = 1.2 \times 10^{-15}$ cm^{2}

REFERENCE

1. S. Kuprianov, M. Tikhomirov, V. Potapov, and P. Karpova, Soviet Physics-JETP, 30, 569 (1956).

THE STUDY OF COLLISION-INDUCED PHENOMENA WITH A DEMPSTER-TYPE MASS SPECTROMETER

By

Harold H.art Harris

A THESIS

Submitted to
Michigan State University
in partial fulfillment of the requirements
for the degree of

DOCTOR OF PHILOSOPHY

Department of Chemistry

1967

To my Parents and Mary

ACKNOWLEDGMENTS

The author wishes to express his sincere appreciation to Dr. Morley Russell for his guidance and encouragement through the performance of this research and the preparation of this thesis. Even though he was at another university during the time most of this investigation was done, he was never too far away to provide helpful advice in times of difficulty.

Many thanks are also due Mr. John Bartelt for helpful discussions of the theoretical portions of this work.

The mass spectrometer used in the present work was purchased in part with funds from the National Science Foundation.

TABLE OF CONTENTS

LIST OF TABLES

LIST OF FIGURES

LIST OF FIGURES - Continued

I. INTRODUCTION

Despite the fact that the Dempster, or 180° deflection, mass spectrometer is very common in analytical mass spectrometry, it has not been applied to the study of collision-induced phenomena. There are two reasons for this. First, since both the ion source and the analyzer are inside the magnetic field, it is comparatively difficult to achieve differential pumping. Second, the effective collision volume is both small and unknown. Its small size means that, at pressures high enough for collisional phenomena to occur in measurable amounts, the ion beam loses a large fraction of its intensity due to collisions with molecules. Under these conditions, the approximations which are usually made in order to interpret the results are no longer valid.

The purpose of this work is to show that meaningful interpretations of collisional phenomena occurring in a 180° spectrometer may be made. Several collision-induced bands have been studied, and the results are comparable to measurements obtained by other means. Scrupulous attention has been given to the measurement of the pressure in the effective collision volume, and the calibration of the pressure gauge.

Unfortunately, the literature of mass spectrometry is not consistent concerning the nomenclature used to describe reactions which occur inside a mass spectrometer. In this thesis, the definitions of these terms will be as follows:

1. secondary process: any process occurring in the spectrometer which requires a collision.
2. collision-induced phenomenon: a process which requires a collision in the spectrometer analyzer tube.
3. ion-molecule reaction: a process which requires a collision in the spectrometer ion source.
4. Aston band: a diffuse peak caused by either a metastable transition or a collision-induced reaction.

II. HISTORICAL

The first mass spectrometer (1,2) was built by the Nobel laureate, F. W. Aston. Ions were produced by a gaseous discharge and separated into a homogeneous energy beam by deflection in an electrostatic field. Then a magnetic analyzer was used to further differentiate them according to their mass-to-charge ratio (m/q). The resolved ion beams darkened the photographic film used for a detector. Almost all of the ions fell on narrow lines, corresponding to the mass-to-charge ratios of the stable isotopes of the gas in the discharge tube.

When the vacuum in the instrument was allowed to deteriorate, diffuse bands were sometimes observed in the spectra (1,2). Although he did not study these bands in detail, Aston recognized their probable origin as being ions which change their mass-to-charge ratio during a collision with a molecule, after electrostatic deflection, but before magnetic analysis.

Aston observed a band at m/q 5.2 in the spectrum of carbon monoxide, and at m/q 0.5 in the hydrogen spectrum. He showed that the particle giving the 0.5 peak was a proton, arising from the dissociation of H_2^+ after it leaves the electric field (2). The explanation of the band at

m/q 5.
ation
the CO
to the
appear
energy

A
Jordan
of 5.14
are sev
double-
electro
netica
the ar
possib
ther f
mass c
about

who c
He st
hydro
gen.

Poter

(1)

m/q 5.2 in CO was also given by Aston, as being the dissociation of CO^+ to give C^+ and O. If the kinetic energy of the CO^+ ion is partitioned between the fragments according to their masses, he reasoned that the resultant band should appear at m/q 5.14 since the C^+ ion would carry 3/7 of the energy of a primary carbon ion, with mass 12.

A subsequent observation of the band by Bainbridge and Jordan (3) in their double-focusing instrument gave an m/q of 5.145 ± 0.002, in agreement with theory. Although there are several ways of achieving double-focusing, a typical double-focusing instrument first separates the ion beam electrostatically, according to velocity, and then magnetically, according to mass. The increased resolution of the arrangement makes more accurate mass determinations possible, and collision-induced bands appear sharper, further facilitating accurate determination of the apparent mass of Aston bands. Mattauch and Lichtblau (4) studied about 30 bands with their double-focusing spectrometer.

Another of the early experimenters was Smyth (5,6), who observed secondary processes with a mass spectrometer. He studied the H_3^+ ion in the high pressure spectrum of hydrogen, and he also observed the bands produced by nitrogen.

An ion of mass m_1 and charge q_1 accelerated through a potential V will possess a kinetic energy given by

$$\tfrac{1}{2}m_1v^2 = q_1V \qquad (1)$$

where v is the velocity of the ion. If the ion then dissociates to produce a new ion of mass m_2 and charge q_2, the kinetic energy of the second ion will be

$$T = \tfrac{1}{2} m_2 v^2 = (m_2/m_1) q_1 V \tag{2}$$

assuming that the kinetic energy lost or gained during the dissociation process is small compared to the kinetic energy possessed by the first ion.

The radius of curvature of an ion in the magnetic field H is

$$R = \left(\frac{c}{qH}\right)\left(2mT\right)^{\frac{1}{2}} \tag{3}$$

where c is the velocity of light, q is the charge of the ion, and m is its mass. Using equation (3), we find the radius of the second, or "daughter", ion to be

$$R = \left(\frac{2Vq_1}{H^2 q_2^2}\right)^{\frac{1}{2}} \left(\frac{m_2^2}{m_1}\right)^{\frac{1}{2}} \tag{4}$$

This is the same radius as that traversed by a primary ion of mass-to-charge ratio $(m/q)^*$, where

$$(m/q)^* = \frac{(m_2/q_2)^2}{(m_1/q_1)} \tag{5}$$

This equation was first derived by Dempster (7) and is widely used in the prediction of the positions of Aston bands. Although it is very useful, equation (5) does not determine the origin of an observed peak, since there is only one observable, $(m/q)^*$.

Hipple and co-workers (8,9,10) were the first to recognize that the diffuse peaks in the mass spectra of hydrocarbons were due to ions which spontaneously dissociate between the electrostatic field and the magnetic analyzer. Hipple also showed that in the Dempster, or 180° deflection, spectrometer (the type used in this study) the bands produced by these "metastable" ions occur at the same position they do in sector-field instruments (10). In addition, Hipple's spectrometer (9,10) was equipped with a means of measuring the energy of the ions causing a metastable peak. This was accomplished by varying the potential of the analyzer with respect to the final slit. The fraction of the original accelerating energy possessed by the fragment ions was obtained by varying the analyzer potential until the metastable peak disappeared. Then, from equation (2),

$$(6) \qquad \frac{m_2/q_2}{m_1/q_1} = \frac{V_2}{V_1}$$

where m_1 and m_2 are the initial and fragment masses, q_1 and q_2 are their charges, respectively, V_1 is the accelerating potential, and V_2 is the retarding potential. This system provides a second equation for Aston bands, and makes the determination of their origins unambiguous. Variations of Hipple's experimental apparatus have been widely used in the study of both metastable ions and collision-induced phenomena.

Henglein and Ewald used a "parabolic" mass spectrometer (invented by Eisenhut and Schutze (11,12)) to study collisional dissociation of both positive and negative ions from a number of gases, including ethylene, carbon dioxide, hydrogen, methane, water, propane, nitrogen, and several isotopically labeled analogs of these substances (13,14). Their apparatus consisted of an ion source where the ions were formed by electron impact and accelerated electrostatically, a collision chamber which was maintained at high pressure, an analyzer which consisted of colinear magnetic and electrostatic fields, and a photographic plate detector. The ions in the beam leaving the collision chamber were deflected by the magnetic field, in a direction perpendicular to their direction of motion, and perpendicular to the field. The magnitude of the deflection was dependent on the mass of the ions, as in the usual magnetic analysis spectrometer. The electrostatic field deflected the ions perpendicular to their direction of motion, but parallel to the field, and separated them according to their energy. The result was a set of spots on the film, the vertical position giving the relative energies of the product ions producing the darkening, and the horizontal position their mass-to-charge ratio.

Probably the most detailed studies of Aston bands have been carried out in the laboratory of C. E. Melton, with a sector-type magnetic spectrometer specially designed for the purpose (15). The source and the analyzer are completely separated, except for the narrow slit which allows the ion beam to enter the analyzer. A separate vacuum system pumps each side of the slit. This apparatus allows the pressure in the analyzer to be varied by two orders of magnitude without seriously changing the source conditions. Because of this almost complete separation of source and analyzer, Melton was able to study the collision of ions of one gas on the molecules of another. He measured the reaction cross sections for the dissociation of carbon monoxide molecular ions in collision with a variety of simple gases (16), as a function of electron energy and as a function of ion kinetic energy. These results showed that the singly charged molecular ion converts its kinetic energy into vibrational energy when dissociating, while the doubly charged molecular ion converts its electronic energy into vibrational energy. Melton also reported a number of collision-induced dissociations in the mass spectra of acetylene (17), methane (18), n-butane and i-butane (19), and formic and deuteroformic acid (20).

Larkin Kerwin and co-workers have used a sector-type magnetic spectrometer (21) to study phosphorus (22) and oxygen (23). In addition, they have published a review of techniques useful in the study of collision processes in a mass spectrometer (24).

There have been several modern reinvestigations of bands studied qualitatively by the early mass spectrometrists, including the band at 0.5 in hydrogen (25,26), the bands in n-butane (27), and in methane (28).

An interesting unresolved controversy appears in the literature concerning the mass spectrum of nitrous oxide. Begun and Landau (29,30) have evidence for some metastable contribution to the band at 20.45 mass units, corresponding to the transition:

$$N_2O^+ + M \longrightarrow NO^+ + O + M \tag{7}$$

Friedman and Irsa (31) have also examined the band, and found no evidence for any metastable contribution. The band was also observed in the present work, and it will be discussed again later.

A photoionization source provides reactant ions with a well-defined energy. Experiments performed with such an ion source can therefore yield more detailed information about the excited states of the reactant ion than the usual electron impact source instrument. Excited states may be of importance to collision reactions. Some experiments using such a source have been done by Chupka and Refaey (32).

Perhaps the most powerful tool available for the study of ion collision phenomena is the tandem mass spectrometer. This device consists of two spectrometers, the mass-analyzed ion beam of the first being used to bombard molecules and produce secondary ions in the source of the second spectrometer. Such a system has been used by Lindholm (33-35), Fedorenko (36), Rourke and co-workers (37), and Abbe and Adloff (38-40), among others.

Since collision bands may occur whenever the instrument pressure is high, they often appear in field-emission spectrometers (41).

The same phenomena which give rise to Aston bands in mass spectrometry may be studied in other ways, which do not involve mass analysis (42-46). A review of these techniques has recently been published by Hasted (47).

Collision-induced phenomena also occur in time-of-flight spectrometers, and some new instrumentation has been devised for their detection (48-50). The detection of neutral fragments is a particularly important advantage of the time-of-flight analysis method.

III. THEORETICAL

A. Measurement of Total Collision Cross Sections

Consider a parallel beam of positive ions of homogeneous velocity passing through a hypothetical gas of solid spherical molecules. If an ion passes within a distance r of a molecule, we shall consider a collision to have occurred. The cross-sectional area σ_T presented by a molecule is therefore

$$(8) \qquad \sigma_T = \pi r^2$$

If there are N molecules of the gas per cubic centimeter, the probability that an ion will collide while moving a small distance δx cm through the gas will be $N\sigma_T\delta x$. If we presume that any such collision removes an ion from the beam (or if we define a "collision" as an interaction that removes an ion from the beam), the amount of beam intensity lost in traversing a distance δx, after starting with an intensity I_0 will be:

$$(9) \qquad \delta I = N\sigma_T I_0 \delta x$$

On integration, we find the intensity after moving a distance L through the gas to be (51):

(10) $$I = I_0\exp(-N\sigma_T L)$$

where σ_T is called the total cross section for collision of the ion in the beam with molecules of the gas.

Applying equation (10) to a Dempster-type mass spectrometer, shown in Figure 1, the ion current measured at the collector is given by

(11) $$I = i\ell Q_i N_1 \eta \exp(-\ell_1 N_1 \sigma_{T_1})\exp(-\ell_2 N_2 \sigma_{T_2})\exp(-\ell_3 N_3 \sigma_{T_3})$$

where i is the electron beam intensity, ℓ is the length of the electron beam (cm), Q_i is the cross section for ionization (cm^2), N_1 is the source pressure (molecules/cm^3), η is a term that includes the ion collection efficiency and also takes into account ions which collide with the slit edges, ℓ_1 is the distance (cm) from the electron beam to the first slit, σ_{T_1} is the average total collision cross section (cm^2) for ions in the source, ℓ_2 is the distance (cm) between the accelerating electrodes, N_2 is the pressure (molecules/cm^3) between the accelerating electrodes, σ_{T_2} is the average total collision cross section (cm^2) for ions between the accelerating electrodes, ℓ_3 is the distance (cm) from the second accelerating electrode to the collector, N_3 is the pressure (molecules/cm^3) in the analyzer, and σ_{T_3} is the total collision cross section (cm^2) for ions in the analyzer. The total collision cross sections, σ_{T_1}, σ_{T_2}, and σ_{T_3} are not identical because they are dependent on

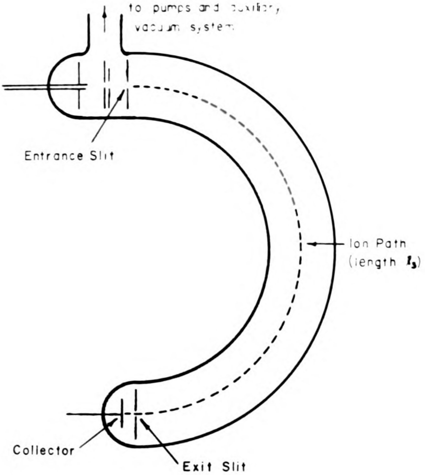

Figure 1(a). The Dempster Mass Spectrometer.

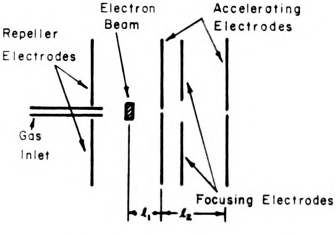

Figure 1(b). Detail of the Ion Source.

energy

variou

of the

the us

σ_{T_1} an

the so

(12)

where L

ion kine

traveled

(13)

where T_0

enters t

electrod

Sin

may be a

(14)

If the p

(15)

Under the

(16) $\frac{dI}{dN}$ =

energy (46), and the ions have different energies in the various portions of the spectrometer. The energy dependence of the total collision cross sections is also the reason for the use of the adjective "average" in the definitions of σ_{T_1} and σ_{T_2}, since the ions are undergoing acceleration in the source. $\sigma_{T_{ave}}$ is better described as

$$(12) \qquad \sigma_{T_{ave}} = \frac{1}{L}\int_0^L \sigma_T(T)\,d\ell$$

where L is the distance the ions are accelerated, T is the ion kinetic energy, and ℓ is the distance the ion has traveled from the first electrode. T is given by

$$(13) \qquad T = T_0 + Eq\ell$$

where T_0 is the kinetic energy possessed by the ion as it enters the accelerating area, E is the field between the electrodes, and q is the charge on the ion.

Since $\ell_1 + \ell_2$ is much smaller than ℓ_3, equation (11) may be approximated, to good accuracy, as

$$(14) \qquad I = i\ell Q_1 N_1 \eta \exp(-\ell_3 N_3 \sigma_{T_3})$$

If the pressure in the spectrometer is uniform,

$$(15) \qquad N_1 = N_2 = N_3 \equiv N$$

Under these conditions, the maximum intensity occurs when

$$(16) \quad \frac{dI}{dN} = 0 = i\ell Q_1 N\eta(-\ell_3\sigma_{T_3})\exp(-N\ell_3\sigma_{T_3}) + i\ell Q_1\eta\exp(-N\ell_3\sigma_{T_3})$$

Solving (16) gives

(17) $$\sigma_{T_3} = \frac{1}{N\ell_3}$$

This provides a convenient determination of the total collision cross section of an ion with its parent gas. Only the analyzer dimension ℓ_3 and the instrument pressure is required, with no standardization with an external system necessary.

B. Measurement of Reaction Cross Sections

The measured ion intensity for ions in an Aston band caused by the reaction

(18) $$A^+ + M \longrightarrow B^+ + C + M$$

may be derived in much the same way we found the intensity of a primary ion, in equation (11). Consider as before a parallel beam of positive ions of homogeneous velocity passing through a gas. In the derivation of equation (11), we considered collisions only as processes which remove ions from the original beam. In fact, there may be several processes which can "destroy" the ions. For instance, they may dissociate, they may exchange charge with the gas molecules, they may abstract a portion of the gas molecules, or they may simply be scattered out of the beam. Each of these processes has a characteristic cross section σ_i.

Clearly,

$$\sigma_T = \sum_{i=1}^{n} \sigma_i \tag{19}$$

The number of particles of the product of reaction i produced will be given by

$$I_i = I_0[1 - \exp(-\ell \sigma_i N)] \tag{20}$$

where I_i is the intensity of the beam of product ions, I_0 is the reactant ion beam intensity, ℓ is the length of the reaction chamber, σ_i is the cross section for reaction, and N is the pressure. Coggeshall (52) has shown that reactions that contribute to an Aston band in a Dempster-type mass spectrometer must occur in a small volume near the entrance to the analyzer (see also Appendix 2). Using Coggeshall's result and equations (10) and (20), we may write down the intensity of the Aston band caused by reaction (18) occurring in a 180° deflection instrument as

$$I_{AB} = i\ell Q_{i_A} N_1 \eta_B \exp(-\ell_1 N_1 \sigma_{T_{1A}}) \exp(-\ell_2 N_2 \sigma_{T_{2A}}) \tag{21}$$

$$\times\ [1 - \exp(-\ell_4 N_4 \sigma_{AB})] \exp(-\ell_3 N_3 \sigma_{T_{3B}})$$

where I_{AB} is the intensity of the band, and the other symbols are as in equation (11), with the subscripts A and B indicating that the constant in question is for the reactant ion A^+ or the product ion B^+, respectively. ℓ_4 is the effective length of the reaction chamber, and σ_{AB} is the reaction cross section (cm^2).

Normally, the product ion B^+ may be formed as a primary ion in the electron beam as well as by the collision-induced reaction. The ratio of the intensities measured for the Aston band and for the primary ion which is the product of the reaction is

$$(22) \quad \frac{I_{AB}}{I_B} = \frac{Q_{1_A} \exp(-\ell_1 N_1 \sigma_{T_{1A}}) \exp(-\ell_2 N_2 \sigma_{T_{2A}}) [1 - \exp(-\ell_4 N_4 \sigma_{AB})]}{Q_{1_B} \exp(-\ell_1 N_1 \sigma_{T_{1B}}) \exp(-\ell_2 N_2 \sigma_{T_{2B}})}$$

assuming that the collection efficiency for the secondary ion B^+ is the same as for the primary ion B^+. In order for the term $\exp(-\ell_3 N_3 \sigma_{T_{3B}})$ to cancel, it must be assumed that $\sigma_{T_{3B}}$ is not a strong function of energy. For the energy range of ions in the usual mass spectrometer, this is probably a good assumption (53).

If the pressure is kept low enough so that only a few percent of the ion beam intensity is lost before the beam enters the analyzer, the first two exponential factors in the numerator will be near unity, as will the two in the denominator. Therefore their ratio will also be near unity, and they will cancel one another. (We can expect this not to be the case only when the pressure is very high or if one of the total collision cross sections is very large). Then

(23) $$1 - \frac{I_{AB}}{I_B}\frac{Q_{1_B}}{Q_{1_A}} = \exp(-\ell_4 N_4 \sigma_{AB})$$

or

(24) $$\ln\left(1 - \frac{I_{AB}}{I_B}\frac{Q_{1_B}}{Q_{1_A}}\right) = -\ell_4 N_4 \sigma_{AB}$$

Using the relationship

(25) $$\ln(1 - x) = -x - \frac{x^2}{2} - \frac{x^3}{3} - \dots \qquad (x < 1)$$

and taking just the first term,

(26) $$\frac{I_{AB}}{I_B}\frac{Q_{1_B}}{Q_{1_A}} = \ell_4 N_4 \sigma_{AB}$$

The ratio $\frac{Q_{1_B}}{Q_{1_A}}$ is obtained from the low pressure mass spectrum of the gas being studied. N_4 is the measured pressure in the collision volume. ℓ_4 is unknown and has not been adequately estimated theoretically (see Appendix 2). In the present study, ℓ_4 was obtained by measuring each of the terms in equation (26) except σ_{AB} and ℓ_4, then using the value of the reaction cross section σ_{AB} for a reaction studied by Kuprianov and co-workers (54), ℓ_4 was determined.

It is of interest to compare the approximations made in the present development with those required by other theoretical treatments of collisional phenomena in mass spectrometry. Most of the quantitative data published to date have been presented as a graph of I_{AB}/N_4 vs. pressure, where the pressure is often approximated by the peak height of an arbitrary primary ion. The development of the theory leading to this treatment of the data is given by McGowan and Kerwin (24) and by Melton (55). McGowan and Kerwin start with the equation (using their notation)

$$(27) \qquad n = n_0 \exp(-\sigma_T L p \ell)$$

where n is the number of parent ions that remain after the original number n_0 have traversed a path length of ℓ cm, σ_T is the total cross section for loss of parents in cm^2, L is the density of molecules per mm Hg pressure at 0^oC, and p is the pressure in mm Hg. They expand the exponential in (27) as a power series and assume that the loss of parents is only a few percent. Then, using just the first term of the series and defining $n_f = n_0 - n$, they find

$$(28) \qquad \sigma_f = n_f/nLp\ell$$

where σ_f is the cross section for the production of a particular product (σ_f corresponds to σ_1 in equations (19) and (20) of the present work). If n_f/n is plotted vs. pressure, the result should be a straight line through the origin, with slope $\sigma_f \ell L$. Metastable contributions to the band would displace the intercept up from the origin. Melton's development is similar, but it is confused by his use of the symbol σ as both a total collision cross section and as a reaction cross section. Both of these derivations require that the collection efficiencies of the primary and secondary ions be equal, and that only a few percent of the original beam intensity is lost while traversing the spectrometer.

In contrast, the theory given here requires only that the ion beam attenuation in the source be small, that the intensity of the band being measured be much smaller than the intensity of the product primary ion peak, that the primary and secondary ion collection efficiencies be equal for the product ion, and that the total collision cross section for the product ion not be a strong function of kinetic energy. Since the source length is typically one to two orders of magnitude smaller than the total length of the ion path, one can expect linear graphs even when the pressure in the instrument is very high.

The treatment of Ackerman and co-workers (56) begins with the equation

$$(29)\quad I^{+} = i^{-}\ell Q_{i} p_{s} \eta \exp(-p_{T} Q_{a} L) = p_{T} S \exp(-p_{T} Q_{a} L)$$

where i^{-} is the electron beam intensity, ℓ its length, Q_i the ionization cross section, p_s is the pressure in the source, and η is the ion collection efficiency; Q_a is the total collision cross section, p_T is the analyzer pressure, and L is the effective length of the tube; S is defined by equation (29). At low electron beam intensities, equation (29) accurately represents the results and permits one to determine Q_a and S. The intensity of an Aston band is given by Ackerman and co-workers as

$$(30) \quad I^{+'} = p_T S[1 - \exp(-p_T Q_a{}' L')]f_1 f_2$$

where $Q_a{}'$ is the cross section for the individual process causing the band, L' is the effective length of the reaction volume, f_1 takes account of the absorption of secondary ions, and f_2 is the secondary ion collection efficiency. At low pressures, $f_1 = 1$. Thus a plot of log I vs. log p_T is, at low pressures, a straight line with slope 2 and whose intercept yields $Q_a{}'f_2$.

Here again we find the necessity of working at pressures low enough so that there is not much loss of secondary ions in the analyzer. Also, their derivation does not allow for varying ratios of source to analyzer pressures, and metastable contributions to the band are not apparent.

IV. EXPERIMENTAL

This study was performed on a Consolidated Electrodynamics Corporation Model 21-103C, 180 degree magnetic deflection mass spectrometer. The instrument has been modified so that a battery power supply can be used to provide the electron accelerating potential when electron energies above 100 volts are desired. Another minor modification allowed ionization efficiency curves (ion current versus electron energy) to be drawn directly with an X-Y recorder. A Honeywell Corporation Model 1508 direct-printing oscillograph was used to record the ion currents. The ultimate vacuum obtainable in the system was approximately 10^{-7} mm Hg.

The gas to be studied could be introduced either through a gold foil leak into the source, or from an auxiliary vacuum system, whose connection to the spectrometer was on the glass line which connects the analyzer tube to the mass spectrometer vacuum pumps (see Figure 2). When an experiment was to be performed, the magnetic valve which isolates the analyzer from the instrument's cold traps was closed. The valve did not make a positive seal, however, and after a sample of gas had been introduced, the mass

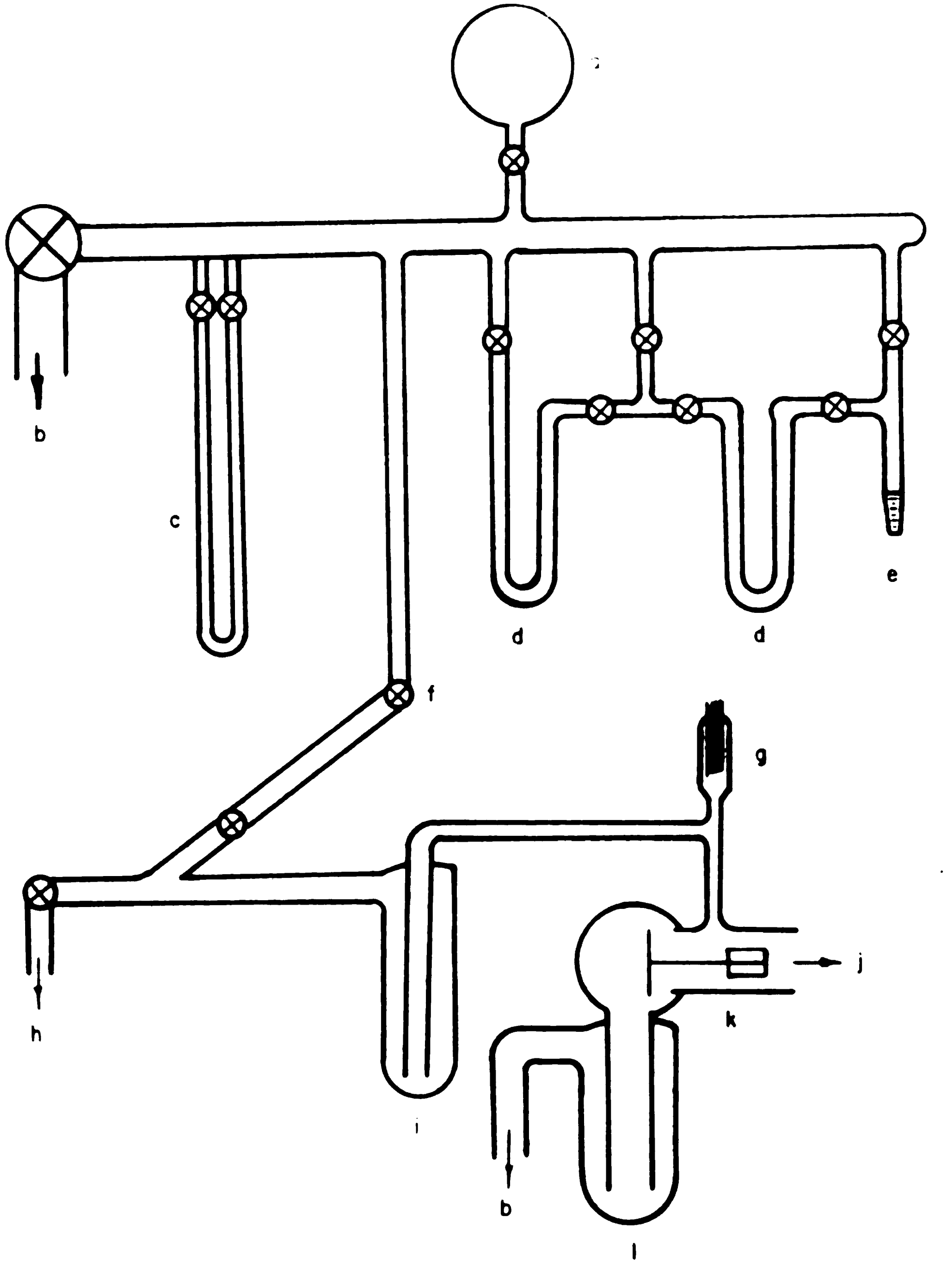

Auxiliary Vacuum System

Figure 2. a. Gas Reservoir; b. Outlet to vacuum pumps; c. Manometer; d. Distillation Traps, e. Gas Inlet; f. Variable Leak; g. Ionization Gauge; h. to Mc Leod Gauge; i. Cold Trap; j. to M.S. Analyzer; k. Magnetic Valve, l. Liquid Nitrogen Trap.

spectrometer vacuum pumps could very slowly reduce the pressure in the analyzer to about 10^{-5} mm Hg, depending on the gas.

During the determination of a particular reaction cross section, the magnetic field was adjusted so that the Aston band was focused at 1000 volts accelerating potential, with a repeller electrode potential of 15 volts. The ionizing current was set at $50\mu A$, and the band intensity was measured as a function of analyzer pressure. Then the magnetic field was reset so that the corresponding primary ion peak was focused at $\left(\frac{q_1}{q_2}\frac{m_2}{m_1}\right)(1000)$ volts, and this peak was studied as a function of pressure. The ratio of these two curves yields the reaction cross section, according to equation (26).

All pressure measurements were made with a VG-1A ionization gauge, calibrated for each gas against an H. S. Martin Co. type M23922A McLeod gauge which was cooled in ice in order to eliminate the Ishii-Nakayama pumping error (57-60).

The cold trap between the McLeod gauge and the system serves to prevent mercury vapor from reaching the ionization gauge and causing erroneous measurements. There is a constant stream of mercury molecules passing from the gauge to the trap, and collecting there. Gas molecules in the system colliding with these mercury molecules tend to be swept away from the McLeod gauge, and the gauge pressure is thus artificially lowered. Although the pumping effect may be avoided merely by cooling the mercury reservoir, and then closing the stopcock at the top of the gauge while the mercury rises to the capillaries (61), this method leaves room for some question as to the gauge temperature to be used in correcting for the effects of thermal transpiration and mercury density change (62). With just the bottom of the gauge in the ice bath, it was found that the mercury temperature could reach as much as $15^{\circ}C$ by the time the gauge was full of liquid.

The apparatus used is shown in Figure 3. The McLeod gauge head was completely surrounded by ice, and the mercury reservoir was kept at $0^{\circ}C$ by the ice-water bath. The system was allowed to cool for several hours before measurements were made. Ice was prevented from obscuring the operator's view of the capillaries by small plastic shields which extend from the viewing port to the gauge. The capillaries were tapped with a glass rod which fits through a hole in the plastic ice container near the viewing port. Measurements of the temperature of the glass tubing containing mercury during a pressure measurement indicate that the mercury temperature never rises above $1^{\circ}C$. No mirror of mercury was visible in the cold trap even after many hours of operation.

The gases used in this study were obtained from The Matheson Company. The carbon monoxide was C. P. grade, the

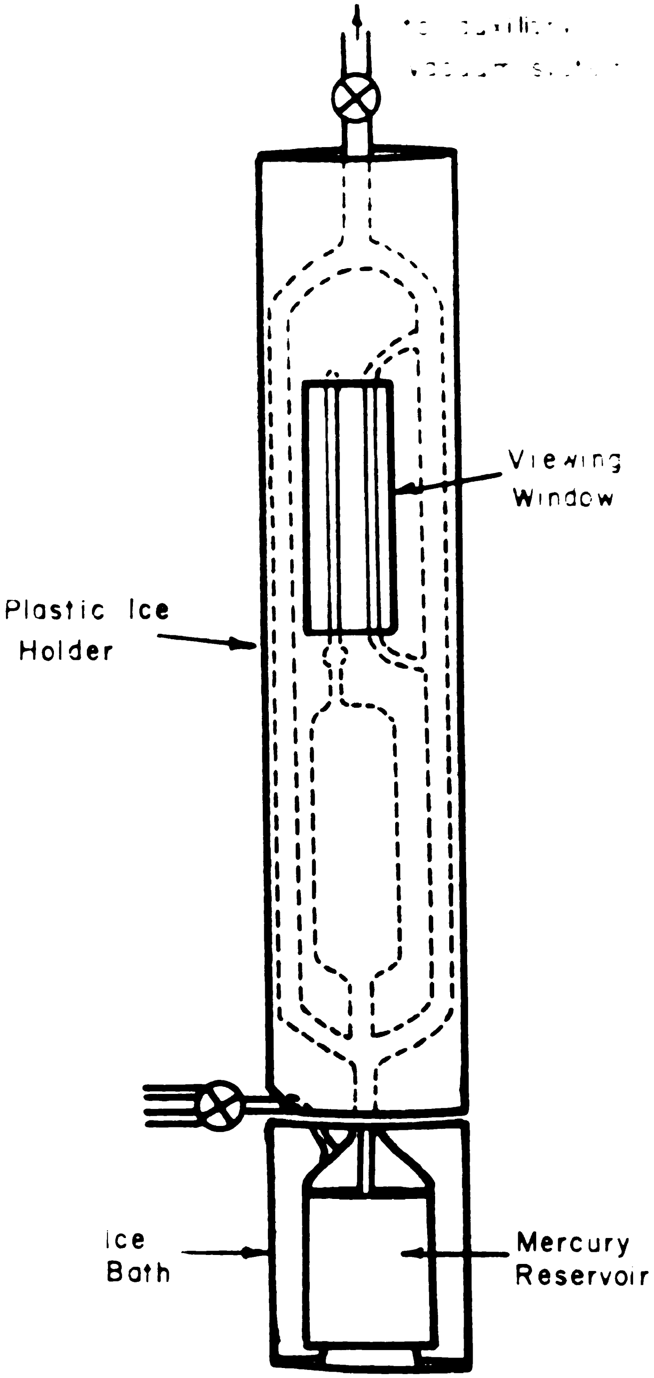

Figure 3. Cooled Mc Leod Gauge.

carbon dioxide was instrument grade, and the argon was prepurified grade. These three gases were used without further purification. The nitrous oxide was 98.0% pure grade. The mass spectrum of the gas as it came from the tank indicated that it was about 2% nitrogen, so the samples used in the study were further purified by freezing them in liquid nitrogen and pumping off the nitrogen gas. The mass spectrum of the compound after this purification step is that given below. The nitrogen gas was high-purity grade and was passed through a purification train consisting of Fieser solution, lead acetate solution, sulfuric acid, calcium chloride, sodium hydroxide, and Drierite. The mass spectra of all of the gases are given below. Spectra compiled by the American Petroleum Institute (63) are listed for comparison.

TABLE 1

Mass Spectra of the Gases

Argon

Mass No.	This Work	API (63) Spectrum No. 1586
18 (H_2O)	0.10	-
20	14.32	12.9
28 (N_2)	0.27	-
32 (O_2)	0.98	-
36	0.37	0.32
38	0.07	0.05
40	100.0	100.0

Carbon Dioxide

		API Spectrum No. 157
12	14.1	6.67
13	0.15	0.09
16	17.1	9.40
22	2.62	-
28	5.03	8.17
29	0.05	0.10
44	100.0	100.0
45	1.25	-
46	0.42	-

Carbon Monoxide

		API Spectrum No. 156
12	6.72	4.71
13	0.068	0.05
14	0.797	0.75
16	3.17	1.67
28	100.0	100.0
29	1.15	1.16
30	0.22	0.22
32 (O_2)	0.102	-

TABLE 1 (Continued)

Nitrogen

Mass No.	This Work	API Spectrum No. 1595
14	13.9	5.18
16 (O)	0.12	-
17 (OH)	0.30	-
18 (H_2O)	0.94	-
28	100.0	100.0
29	0.755	0.73

Nitrous Oxide

		API Spectrum No. 96
14	12.0	9.3
15	0.084	-
16	4.07	2.6
18	0.087	-
28	11.6	- ?
29	0.10	-
30	28.9	27.8
44	100.0	100.0
45	0.80	0.7
46	0.17	0.2

V. RESULTS

A. Carbon Monoxide

The carbon monoxide system is the most important of those studied in the present work because the reaction

$$(31) \qquad CO^+ + CO \longrightarrow C^+ + O + CO$$

was used in conjunction with a literature value for the reaction cross section to determine the effective length ℓ_4 of the collision volume. This instrumental parameter was used in the computation of all the other cross sections from the experimental data. The reaction (31) was chosen for the calibration because it has a large cross section and because the absolute cross section has previously been measured.

Figures 4, 5 and 6 represent the variation with pressure of three of the primary ions in carbon monoxide. In agreement with equation (11), and typical of the primary ions, they contain a linear increase with pressure where the pressure is low, and an exponential decrease from this behavior when the pressure is high. Application of equation (17) yields the total collision cross sections for CO^+, O^+, and C^+ in CO as 2.4×10^{-16}, 5×10^{-17}, and

1.8×10^{-16} cm^2, respectively. There are no values in the literature with which to compare these results.

Figures 7 and 9 display the behavior of typical collision peaks. As is predicted by equation (21), the intensity increases with the square of the pressure at low pressure and decreases exponentially with pressure when the pressure is high. The low pressure dependence is not as clearly recognizable as it is in the case of primary ions, because, when the pressure is high enough to cause a measurable number of reactions, the attenuation of the ion beam in the analyzer is **considerable.**

Figure 8 (circled points) was used for the determination of the length ℓ_4. The slope of this graph is 3.00 mm^{-1}, and using the low pressure mass spectrum of carbon monoxide (Table 1) and the cross section of Kuprianov et al. (54) of 1×10^{-17} cm^2, this yields a value for ℓ_4 of 0.568 cm. Therefore ℓ_4 is only 1.42% of ℓ_3, in agreement with hypothesis.

It was on this basis that the value of Kuprianov et al. (54) was chosen instead of the alternate measurement of 2×10^{-18} cm^2 by Melton and Wells (16). The latter value leads to $\ell_4 = 2.84$ cm. Such a large effective collision volume violates the assumption that ℓ_4 is small compared to ℓ_3, which is implicit in equation (21). This in turn would cause deviations from linear behavior in the graphs of the ratio of the Aston band intensity to the corresponding primary product ion (Figures 8, 10, 14, 17, 20 and 23). These deviations were not observed. The rough calculation of ℓ_4 in Appendix 2 also would preclude such a large value. It should be realized that the reaction cross sections reported in the present work are relative to the value chosen for the calibration reaction.

In order to test whether the analyzer was at pressure equilibrium, and therefore whether the ionization pressure gauge reading was meaningful, the same band was restudied using the conventional gas inlet system. Since the gas leaks directly into the source chamber when the conventional inlet is used, the measured ion intensities were systematically higher than when the auxiliary inlet was used, as can be seen by comparing the "triangle" points in Figures 6 and 7 with the circled points, which were obtained using the auxiliary inlet. (Through the remainder of the figures, circled points will indicate data obtained with use of the auxiliary inlet while points in triangles were measured using the conventional "gas" inlet.) The intensity ratio of interest, Figure 8, is not appreciably changed, however, indicating that the physical position of the gas inlet was not affecting the pressure in the effective collision volume. The cross section as measured with the gas inlet is 8.9×10^{-18} cm^2.

The slight increase in ion current which results from use of the conventional gas inlet was used to advantage in measurement of the band at m/e 10.28 resulting from

(32) $CO^{+2} + CO \longrightarrow C^{+} + (O^{+}) + (CO^{+})$

The intensities measured with the auxiliary inlet were slightly low for accurate determination of the reaction cross section. The results are summarized in Figures 9 and 10. The cross section for reaction (31) is found to be 1.39×10^{-16} cm^2, which is considerably larger than the 7×10^{-17} cm^2 value of Melton and Wells (16). The discrepancy is believed to be a systematic one, resulting from the use of the value of Kuprianov *et al.* for the calibration reaction. Their cross sections are five times larger than those of Melton and Wells. The only other value in the literature which is pertinent to the present discussion is the value of Kuprianov (64) of 2.0×10^{-16} cm^2 for the reaction

(33) $CO^{+2} + Ne \longrightarrow C^{+} + O^{+} + Ne$

This result is very confusing when viewed in light of the results of Melton and Wells. Melton and Wells studied the collision-induced dissociation of CO^{+2} into C^{+} and O, with a series of molecular targets, and showed the cross section for neon to be over one thousand times smaller than that for CO. On this basis, we would have to conclude that Kuprianov would measure a cross section in excess of 2×10^{-13} cm^2 for reaction (32)!

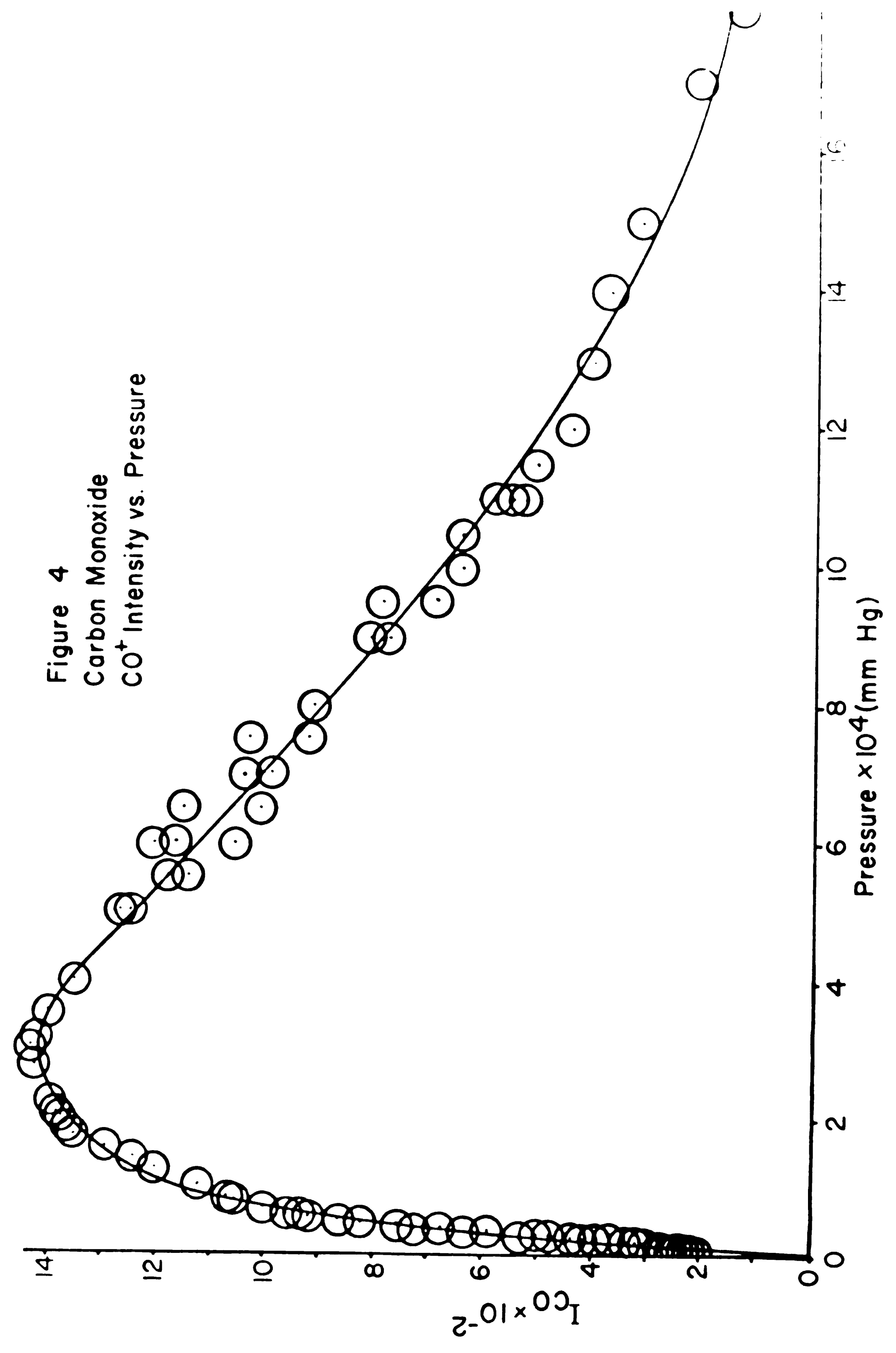

Figure 4
Carbon Monoxide
CO^+ Intensity vs. Pressure

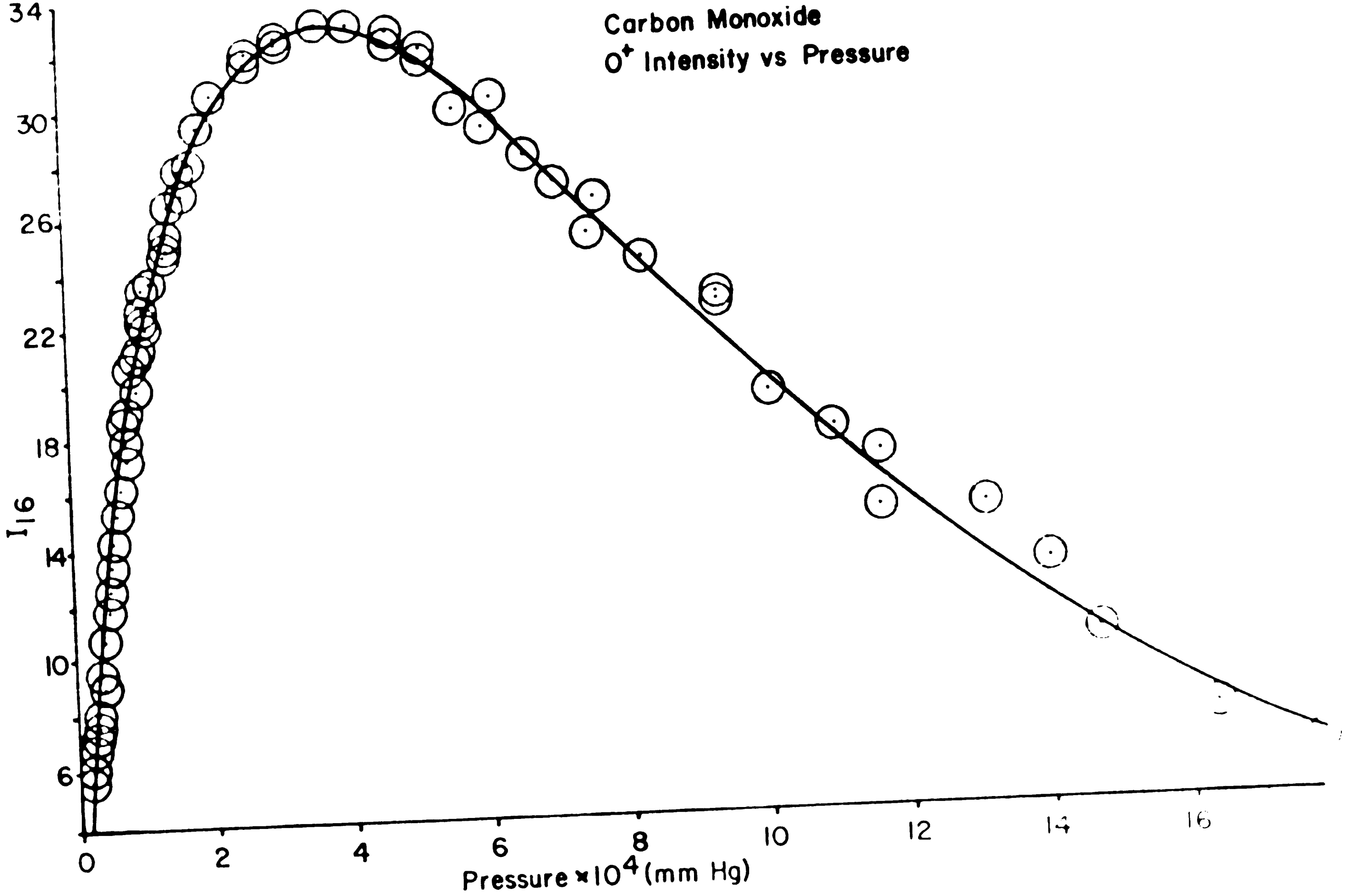

Figure 5
Carbon Monoxide
O^+ Intensity vs Pressure

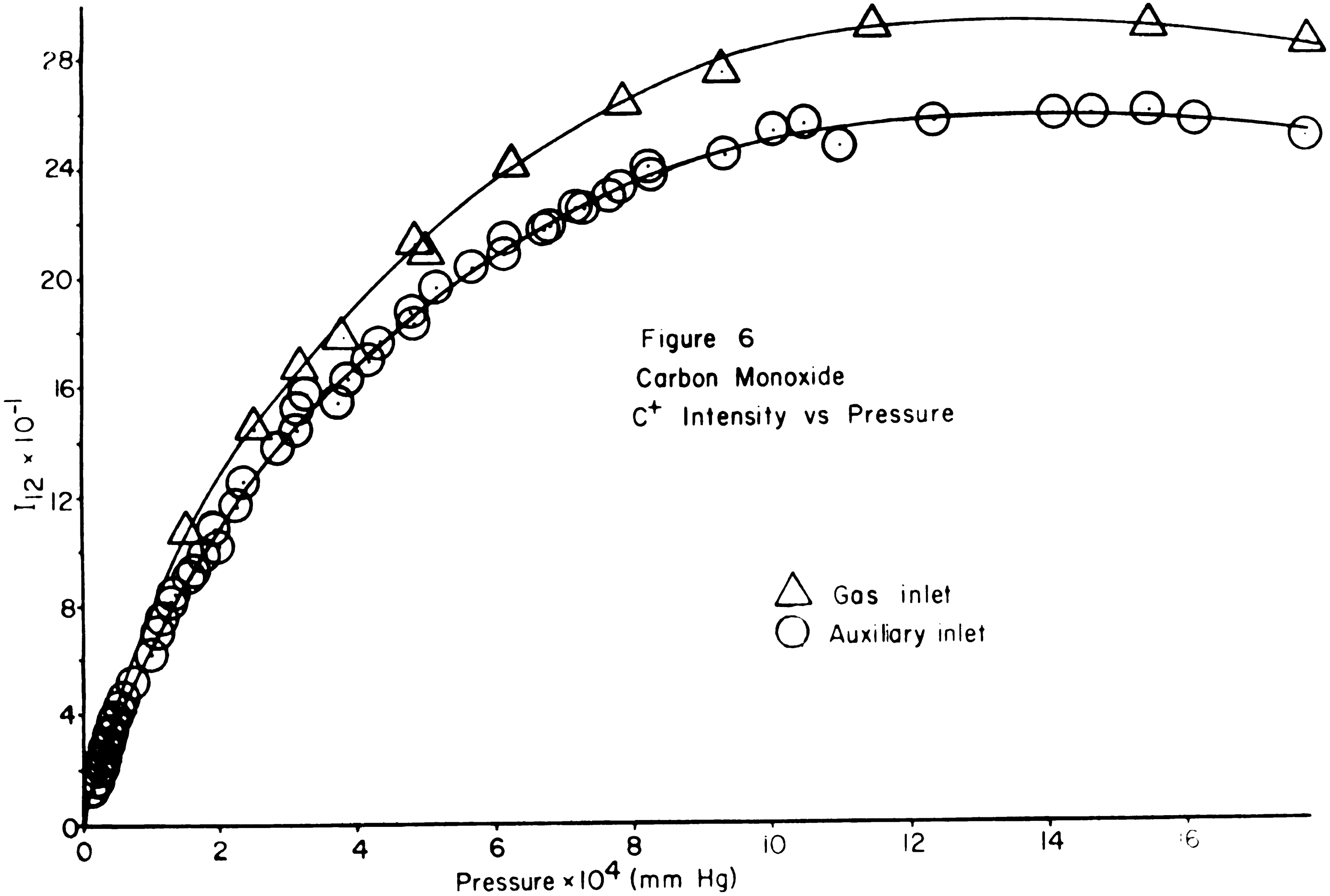

Figure 6
Carbon Monoxide
C^+ Intensity vs Pressure

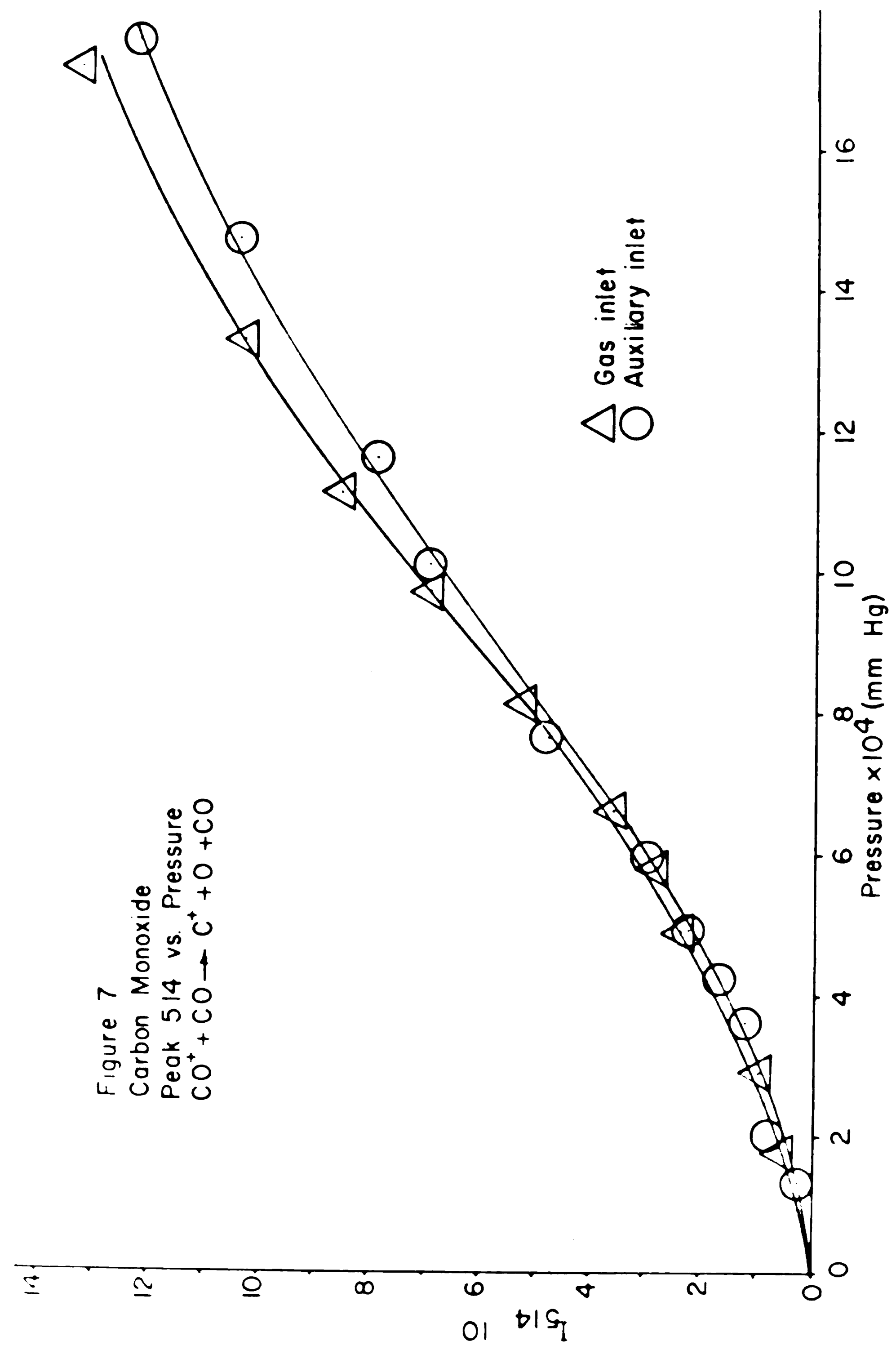

Figure 7
Carbon Monoxide
Peak 514 vs. Pressure
$CO^+ + CO \rightarrow C^+ + O + CO$

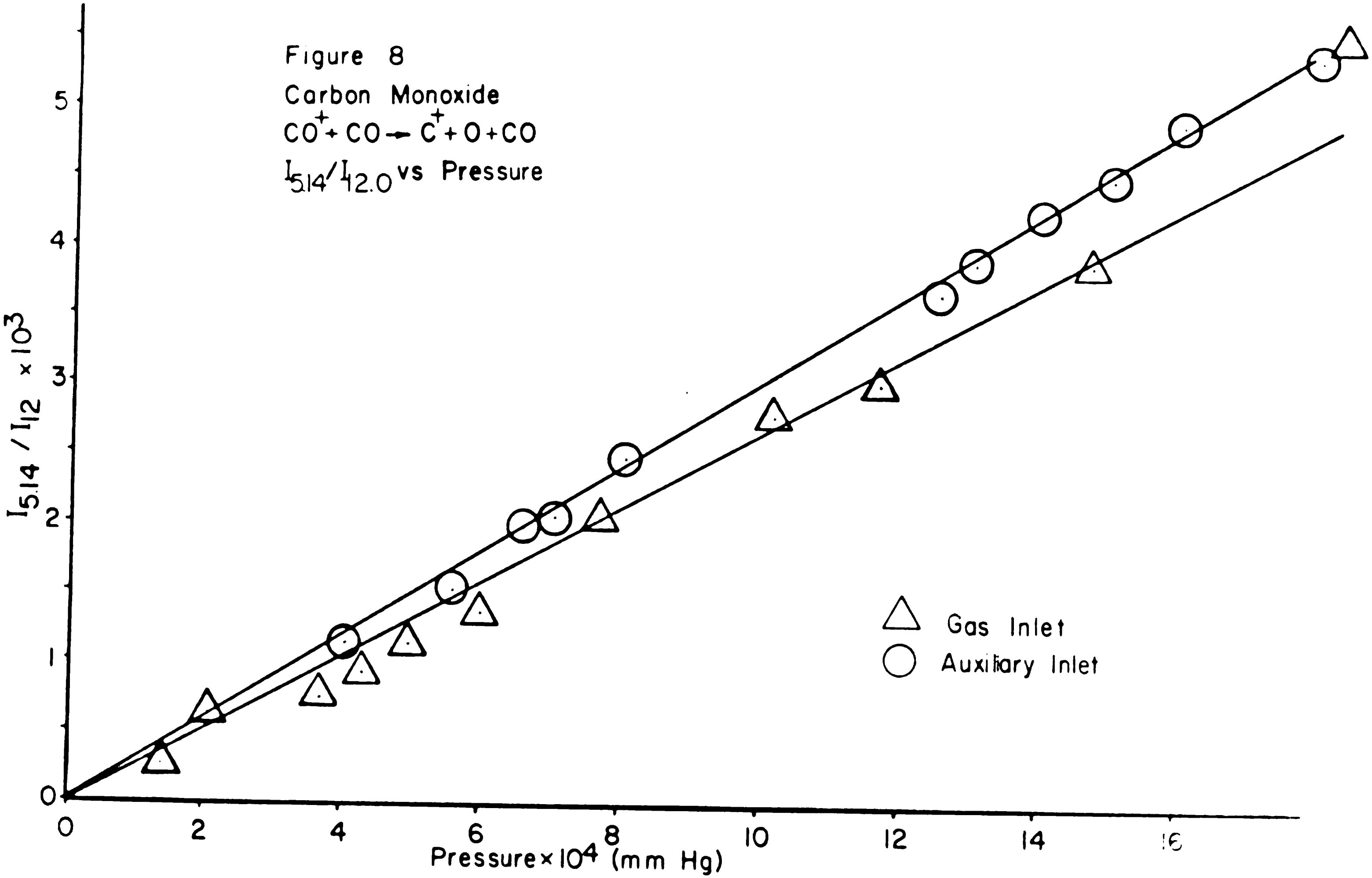

Figure 8
Carbon Monoxide
$CO^+ + CO \rightarrow C^+ + O + CO$
$I_{5.14}/I_{12.0}$ vs Pressure

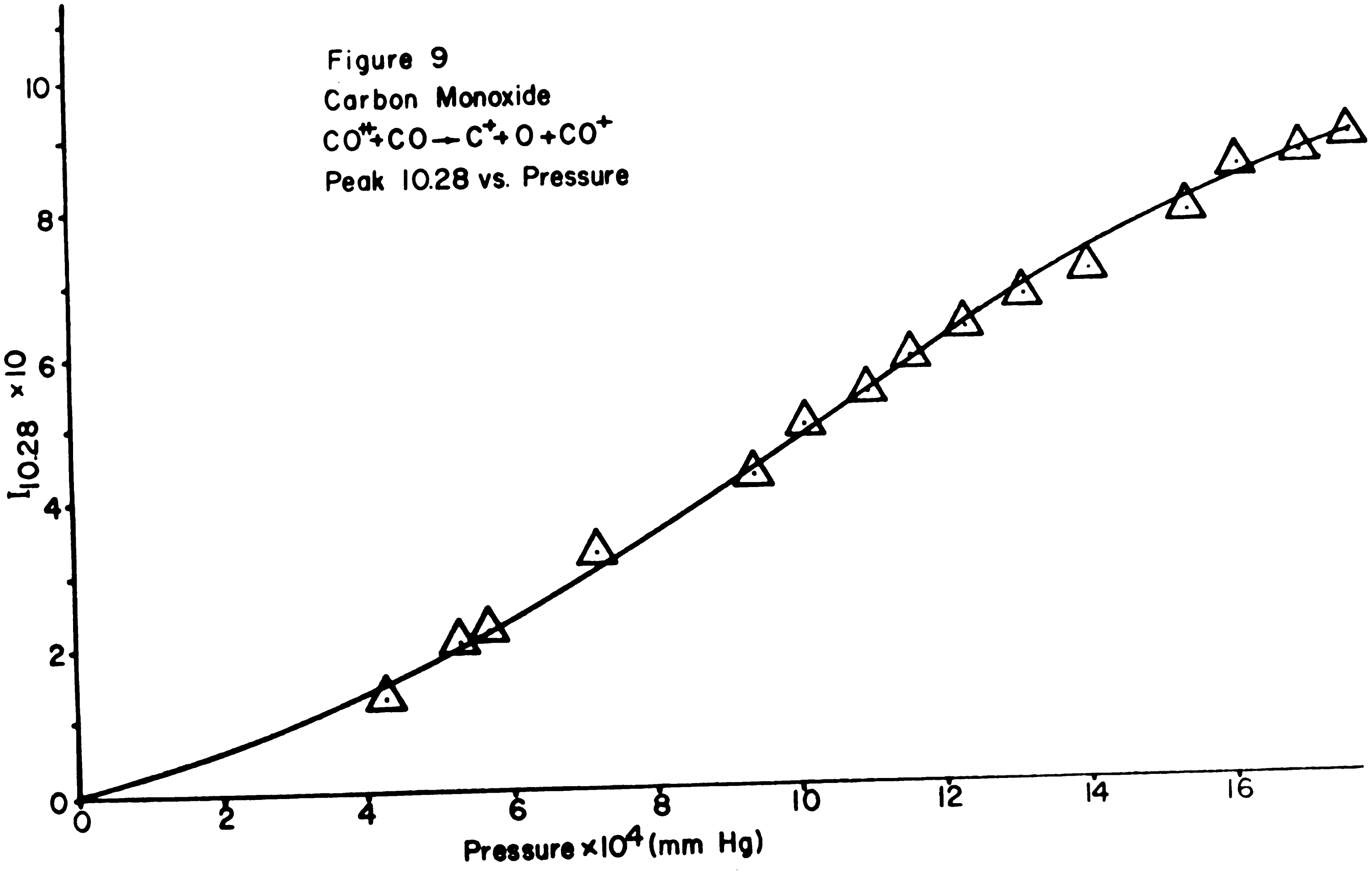

Figure 9
Carbon Monoxide
$CO^{++} + CO \rightarrow C^{+} + O + CO^{+}$
Peak 10.28 vs. Pressure

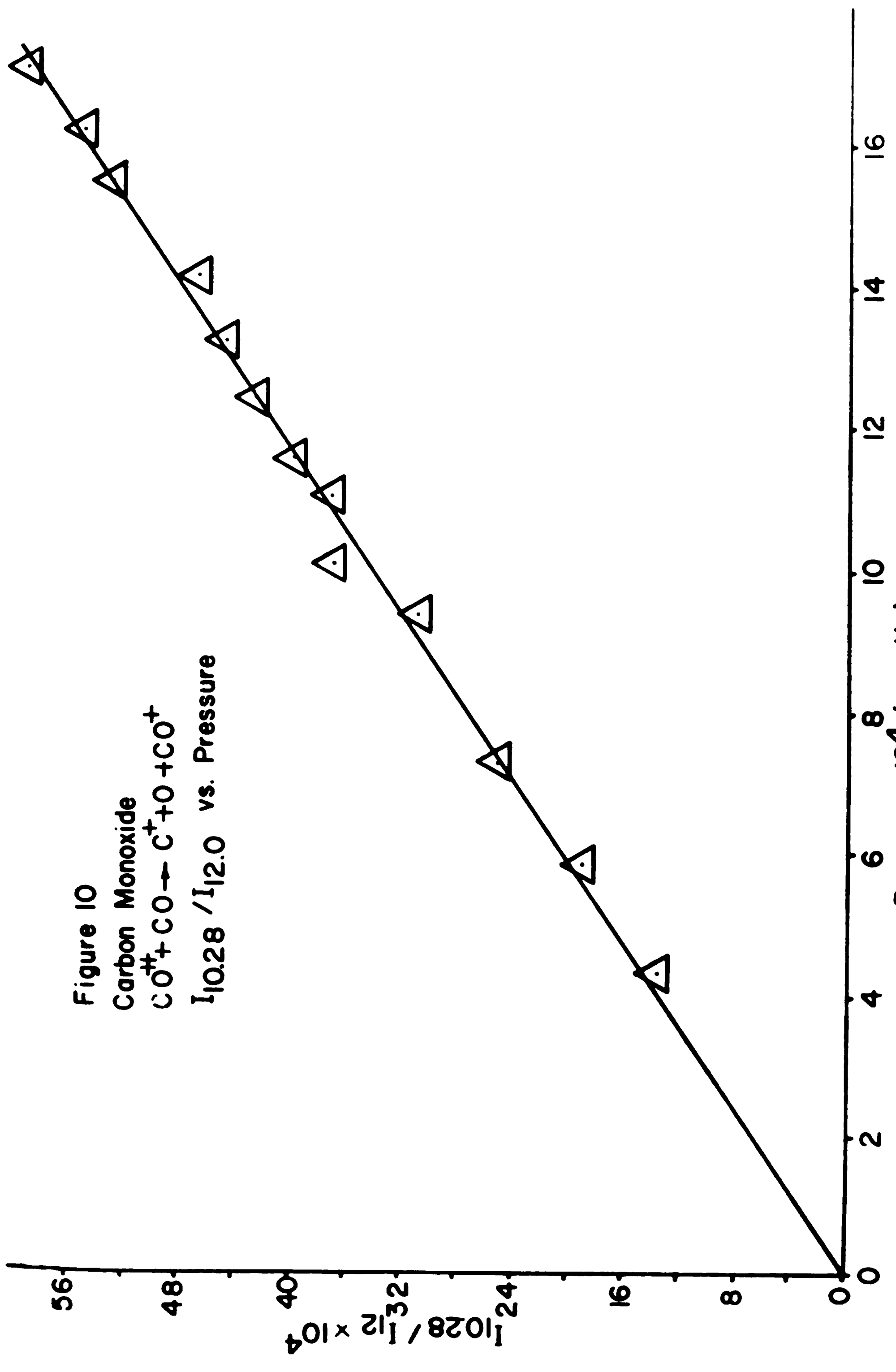

Figure 10
Carbon Monoxide
$CO^{++} + CO \rightarrow C^{+} + O + CO^{+}$
$I_{10.28}/I_{12.0}$ vs. Pressure

B. Argon

The Aston peak technique can be of use in the measurement of charge transfer cross sections, but it is limited to reactions in which the ions accelerated in the source retain at least some of their charge. For instance, the following reactions could theoretically produce Aston bands:

(34) $Ar^{+2} + Ar \longrightarrow Ar^{+} + Ar^{+}$

(35) $Ar^{+3} + Ar \longrightarrow Ar^{+2} + Ar^{+}$

(36) $Ar^{+3} + Ar \longrightarrow Ar^{+} + Ar^{+2}$

(37) $Ar^{+2} + Ar \longrightarrow Ar^{+3} + Ar^{-}$

Reactions which neutralize the bombarding ion are not detected because the neutral fragments are not collected. A search was made for evidence of reactions (35) and (36), but neither of the corresponding bands was detected, presumably because of the very small cross section for triple ionization of argon (65). Reaction (37) has a very low cross section at low energies and is not observed in mass spectrometers (66).

The band produced by reaction (34) appears at m/q 80, and there is the possibility of interference with the ion Ar_2^{+}, which may be produced by collision of an argon ion with a molecule in the source (67). However, the band disappears when the electron energy (uncalibrated) is lowered below about 50 volts, which is somewhat higher than the appearance potential of Ar^{+2} (43.38 e.v.) but much higher than the appearance potential of Ar^+ (15.76 e.v.) (68). An exact appearance potential measurement was not feasible because of the low intensity of the Aston band. The band intensity is also observed to decrease as the electron energy is increased above 130 volts, as does the intensity of the peak at m/q 20, due to Ar^{+2}.

The present experimental section is the only one not performed at 70 volts electron energy. It was done at 130 volts in order to maximize the band intensity.

Figures 11 and 12 yield the total collision cross section for the doubly and singly charged argon cations. They are 1.22×10^{-15} and 2.20×10^{-15} cm^2, respectively. Cramer (69) has measured the total collision cross section for Ar^+ on Ar to be 4.0×10^{-15} cm^2 at an ion energy of 400 e.v. He found it to consist of a charge transfer cross section of 2.0×10^{-15} cm^2 and an elastic scattering cross section of 2.0×10^{-15} cm^2. Although this value is within a factor of approximately three of the results of the present work, even this agreement is largely fortuitous. The reason for this is the difference in experimental methods. Cramer's results were obtained using a total charge collection technique which collected nearly all of the "slow" ions produced when a beam of argon ions collided with a sample of argon gas. By contrast, the Aston peak technique, in measuring the disappearance of charge from the original beam, excludes not only ions that are scattered a very small angle out of their normal flight path, but also those which have lost a small fraction of their momentum. One would expect the results from two such different methods to differ greatly, but a similar effect can be operative even when the apparatuses in use are very similar. A relatively small difference in experimental parameters could cause a large change in the "resolution" of the equipment. By "resolution" is meant the ability of the apparatus to detect a change in the velocity or momentum of an ion and register it, therefore, as "scattered." Because of the differences in the resolution of various instruments, it is a common practice for each investigator to normalize his results to a commonly accepted value for the cross section of an easily measured reaction. The lack of this type of normalization in the comparison of the values in the present work to values in the literature will cause the differences between them to sometimes be very large. In order to avoid some of these difficulties, at least in the literature of the Aston band technique, it is here proposed that subsequent results be reported relative to the cross section for the collision-induced dissociation reaction (31) of carbon monoxide.

The pressure dependence of the m/q 80 band is displayed in Figure 13. It exhibits the second-order behavior at low pressure which is common to all of the collision bands in the present work. Also of interest is the coincidence of the lines formed by points measured with the two inlet systems. This is further evidence that the spectrometer is near pressure equilibrium even when the gas is leaked into the source.

The ratio of the Aston band at m/q 80 to the peak at m/q 40 is plotted in Figure 14. The slope of the straight line, which is independent of the position of the gas inlet, yields a value of 3.56×10^{-16} cm^2 for the cross section of reaction (34). Since all of the experiments in the present work were performed at 1000 volts accelerating potential, the kinetic energy of the initial (doubly charged) ion is 2000 e.v.

Using the Aston peak technique in a magnetic sector mass spectrometer, Weiner, Hertel, and Koski (70) measured the cross section for the partial charge transfer from Ar^{++} to its parent gas to be 0.6×10^{-16} cm^2 at 2000 e.v. rising to 2.0×10^{-16} cm^2 at 6000 e.v. Hasted and co-workers (71) also have measured this cross section, employing a collision chamber technique and collecting the slow ions produced when the doubly charged ions pass through the argon gas sample. However, this method does not discriminate between reaction (34) and the reaction

$$(38) \qquad Ar^{+2} + Ar \longrightarrow Ar + Ar^{+2}$$

Since (38) is a resonant process, it is likely that it has a high cross section at low energy, and this may account for the high value of $2.4 \times 10^{-15} \pm 10\%$ cm^2. A later

urement in the same laboratory (45) was reported, and
his case the results were separated into the contribu-
s from reactions (34) and (38), and those were found
be 2.0 x 10^{-16} and 6.6 x 10^{-16} cm^2 ± 15%, respectively.
sum of the cross section (38) and half of (34) are
excellent agreement with the measurement of Flaks and
olov'ev (72) of 7.8 x 10^{-16} cm^2. (The reason for summing
he cross sections in this way is that the slow ion collection method measures the total cross section for charge production in the target gas, and this amounts to the cross section for production of dipositive ions plus half of the cross section for production of simple ions.) It is felt that the later paper by Hasted and co-workers (45) and the result of Flaks and Solov'ev (72) represent the best experimental values in the literature for the partial charge transfer reaction, and although there are a number of other papers on charge transfer reactions in argon, these will not be mentioned here. Citations of these papers may be found in references (45) and (72).

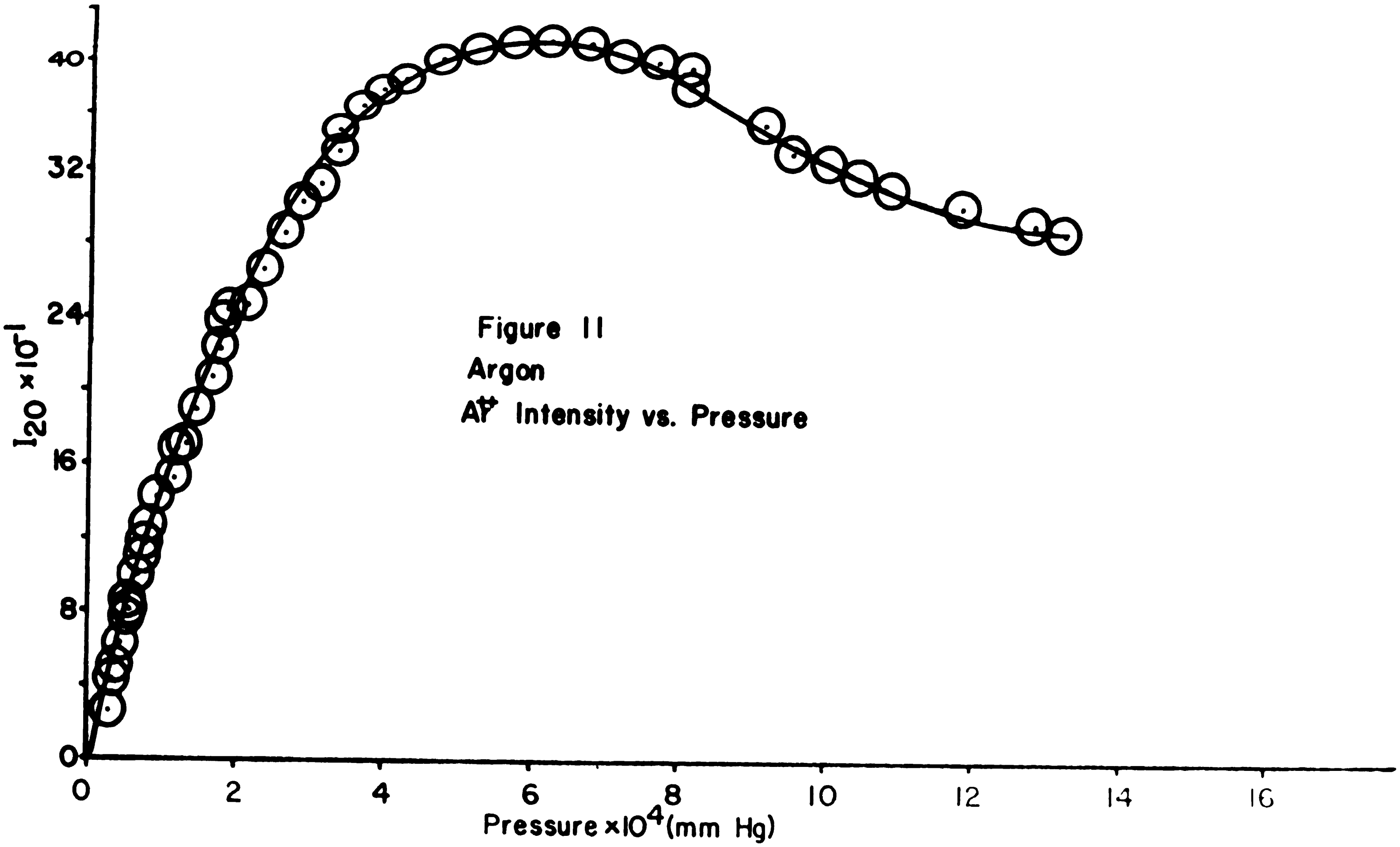

Figure 11
Argon
Ar$^+$ Intensity vs. Pressure

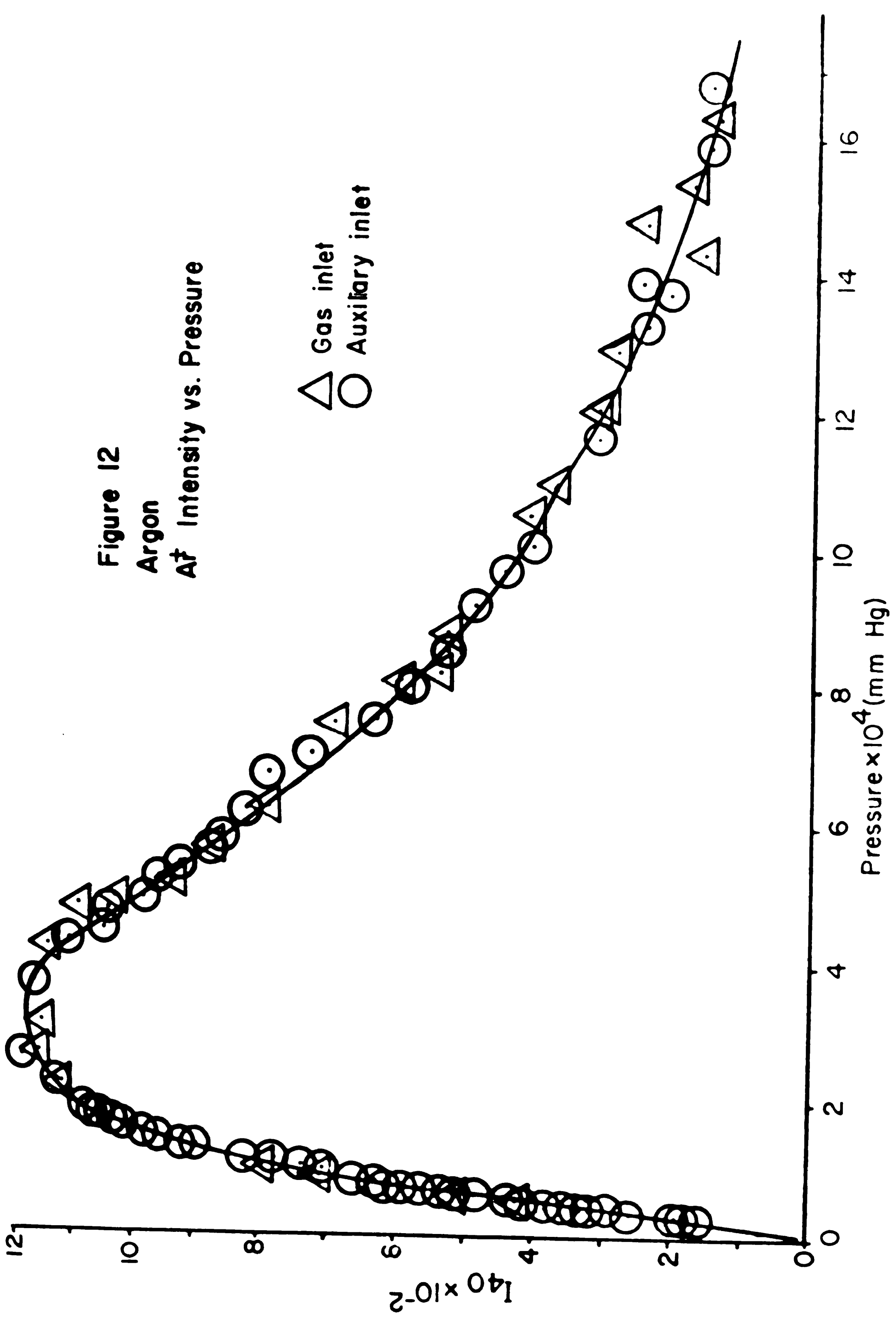

Figure 12
Argon
A$^+$ Intensity vs. Pressure

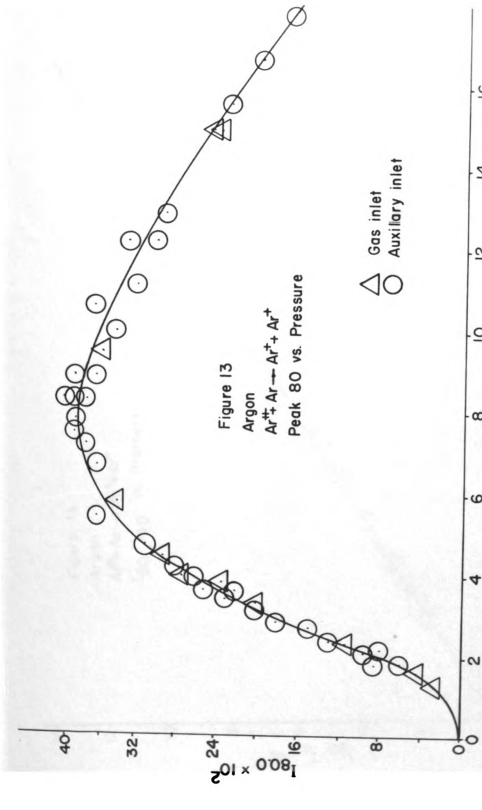

Figure 13

Argon

$Ar^{++} + Ar \rightarrow Ar^{+} + Ar^{+}$

Peak 80 vs. Pressure

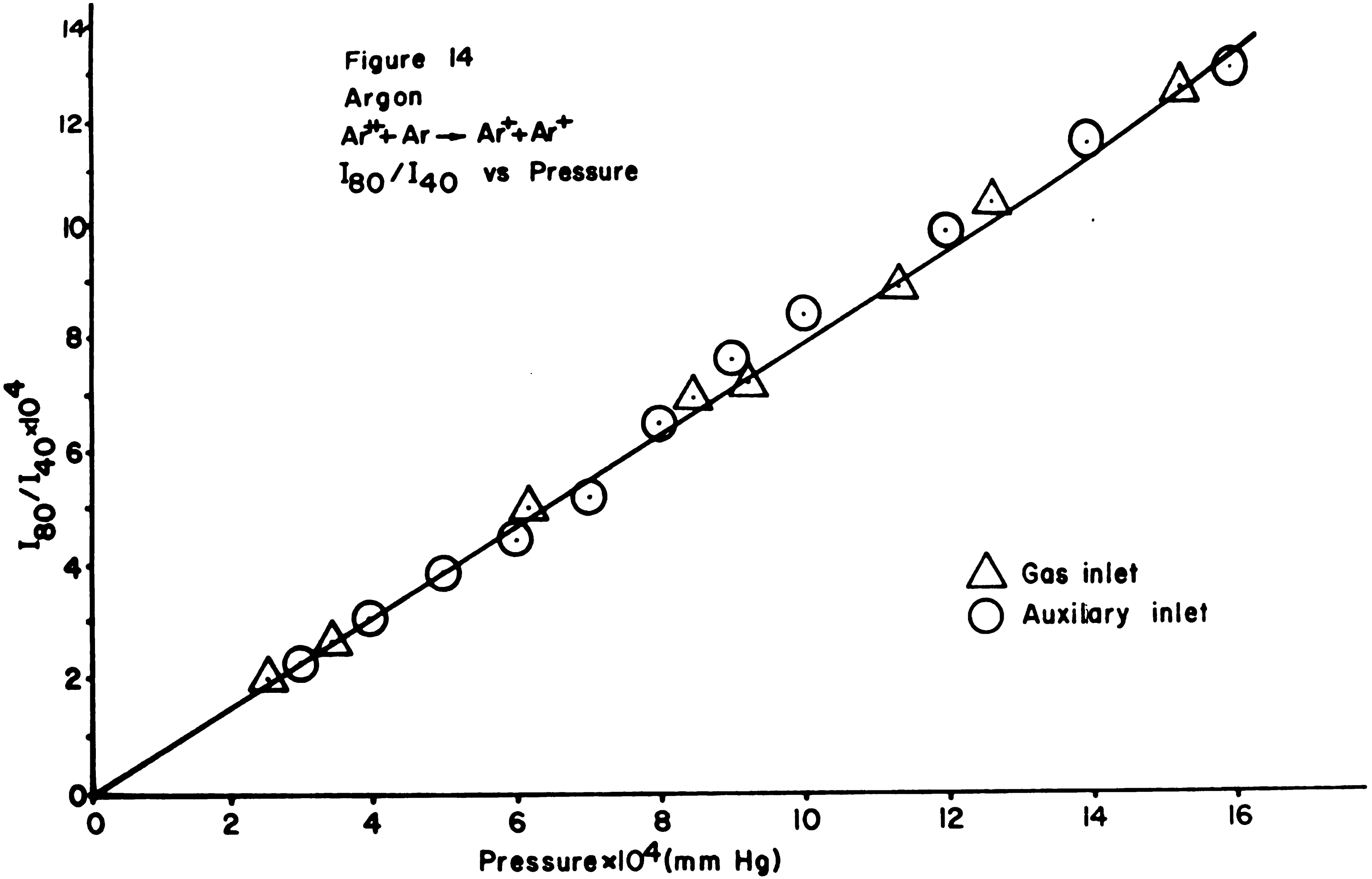

Figure 14
Argon
$Ar^{++} + Ar \rightarrow Ar^{+} + Ar^{+}$
I_{80}/I_{40} vs Pressure

C. Carbon Dioxide

The CO^+ and CO^{+2} ions produced by the ionization and fragmentation of carbon dioxide should undergo the same collision-induced reactions as the same ions produced by the ionization of carbon monoxide. Therefore, one might expect all of the Aston bands which appear in the high pressure mass spectrum of CO to also be found in the spectrum of CO_2. However, an examination of the analytical spectra of these gases (Table 1) shows why some of the bands are not present. The intensity of an Aston band is proportional to the abundance of the reactant ion in the source. The m/q 28 peak in carbon dioxide is only about 3% of the total ionization of the molecule (the sum of the ion intensities) whereas the same ion accounts for about 90% of the ionization in carbon monoxide. At a given pressure, then, the Aston peaks resulting from the dissociation of CO^+ ions would be about 30 times less intense in CO_2 than in CO.

The m/q 14 peak, due to CO^{++} ions is absent from the spectrum of CO_2. Such an ion would have to be produced by the dissociation of the ion CO_2^{++}. Since the two positive charges could be separated by the formation of two charged species, the doubly charged ion is not produced, at least not in measurable amounts. As a result, the Aston band at m/q 10.28 which was studied in carbon monoxide, was not visible in CO_2.

The m/q 5.14 peak, due to the reaction

$$(39) \qquad CO^+ + CO_2 \longrightarrow C^+ + O + CO_2$$

was not large enough for study with the auxiliary inlet, but the use of the gas inlet increased the intensity enough so that a quantitative measurement was possible. However, introduction of gas directly into the source causes the source pressure to be higher than the analyzer pressure, and therefore one of the conditions (equation 15) used for the derivation of the expression (equation 17) for the measurement of total collision cross sections was violated. The development of the theory for the measurement of reaction cross sections does not require that the entire mass spectrometer be at one pressure, but only that the absorption of the ion beams in the source be small. Using the same equations as previously, Figure 17 yields 6.57×10^{-17} cm^2 for the cross section of reaction (39).

It will be noticed that there is a non-zero intercept in Figure 17, indicating a metastable contribution to the peak. This was the only such behavior observed in the bands studied, and it is believed to be an artifact, arising from a systematic error in the calibration of the pressure gauge of approximately 4×10^{-5} mm Hg. The reason for the necessity of this supposition is the nature of the reactant ion, CO^+. Being a simple diatomic ion, it would seem that there would be no energy levels capable of storing the dissociation energy for as long as 10^{-6} seconds, the approximate time that the ion spends in the source.

Although there are no previous measurements in the literature for the cross section of reaction (39), one might well be surprised to find that this cross section is more than six times larger than that for the same reaction when carbon monoxide is the target gas. Certainly the difference in molecular sizes cannot account for this large difference in cross section. It must be remembered, however, that the reactant ions in the two cases are not identical. One of them was produced by the direct electron impact ionization of carbon monoxide while the other was the result of the unimolecular dissociation of CO_2^+.

Potapov (73) has shown that such differences in the preparation of the reactant ions may affect the cross section for their collision-induced dissociation. He studied the reaction

$$(40) \qquad CO^+ + Ne \longrightarrow C^+ + O + Ne$$

and found the cross section to be 1.75 times larger when the initial ion was produced by dissociation of CO_2^+ than when it was produced by the ionization of CO.

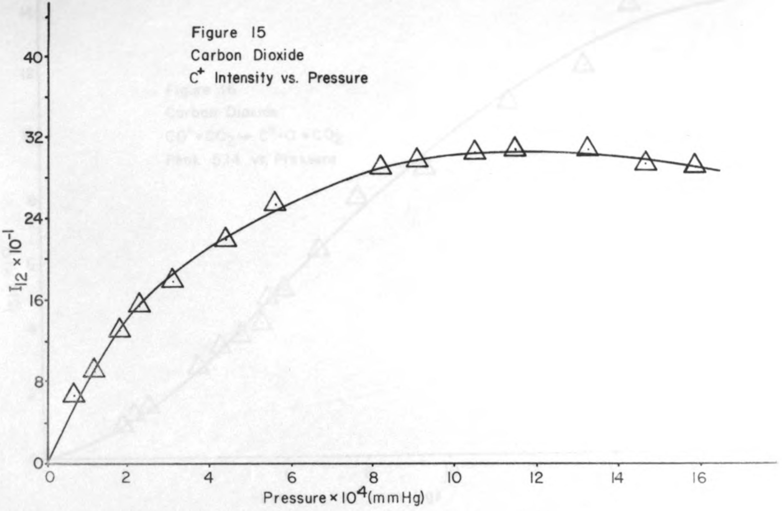

Figure 15
Carbon Dioxide
C^+ Intensity vs. Pressure

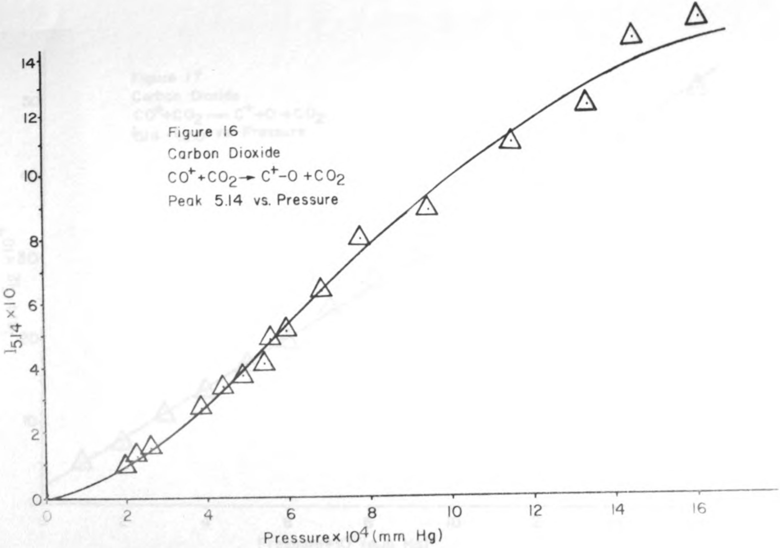

Figure 16
Carbon Dioxide
$CO^+ + CO_2 \rightarrow C^+{-}O + CO_2$
Peak 5.14 vs. Pressure

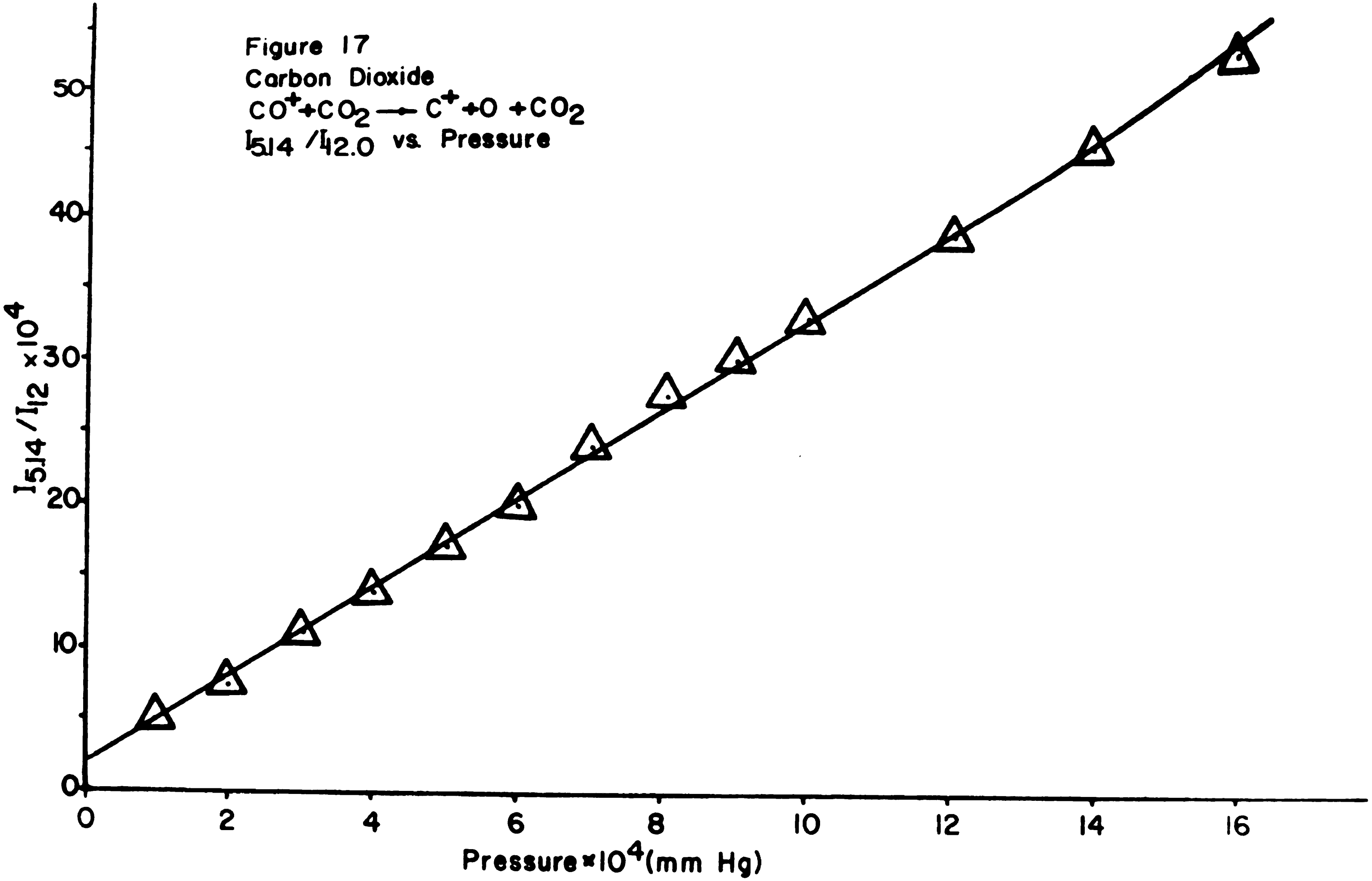

Figure 17
Carbon Dioxide
$CO^+ + CO_2 \rightarrow C^+ + O + CO_2$
$I_{5.14} / I_{12.0}$ vs. Pressure

D. Nitrogen

The only Aston band which was detectable in the nitrogen system arose at m/q 7.0 from the reaction

(41) $$N_2^+ + N_2 \longrightarrow N^+ + N + N_2$$

Since this Aston band coincides with the possible ion N^{+2}, there was some concern that part of the measured band intensity could be contributed by the doubly charged atomic ion. Such a contribution would be first order in pressure, and would appear as a non-zero intercept in the graph of the ratio of the reaction peak to the product ion peak (Figure 20). Absence of such a contribution indicates that the N^{+2} ion is not interfering with these measurements.

The slope of the straight line in Figure 20 yields a cross section for reaction (41) of 3.52×10^{-17} cm^2. Although there have been numerous studies of charge-transfer reactions in nitrogen (40), (70), (74), there apparently has been no previous study of the collision-induced dissociation of N_2^+.

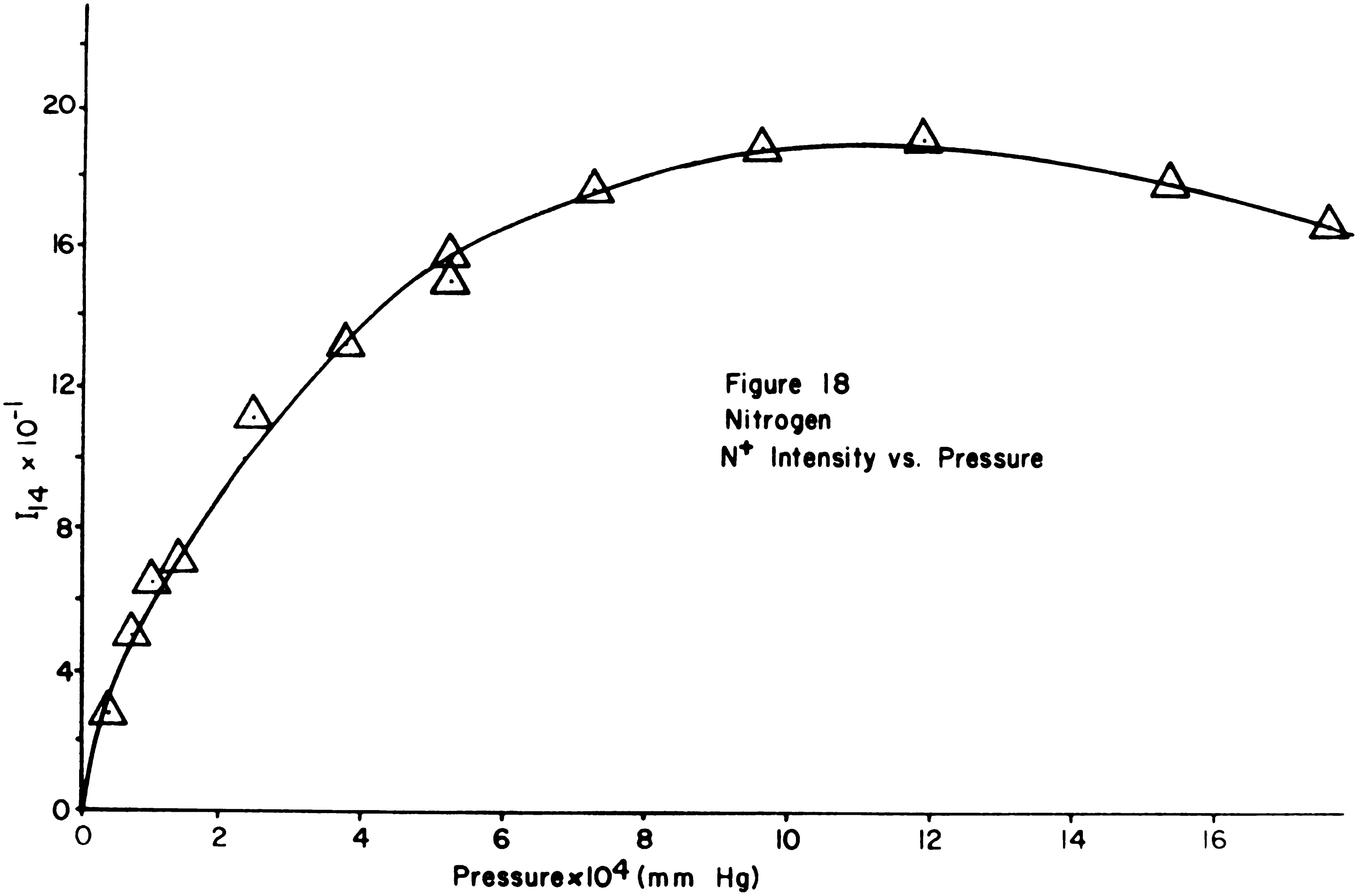

Figure 18
Nitrogen
N^+ Intensity vs. Pressure

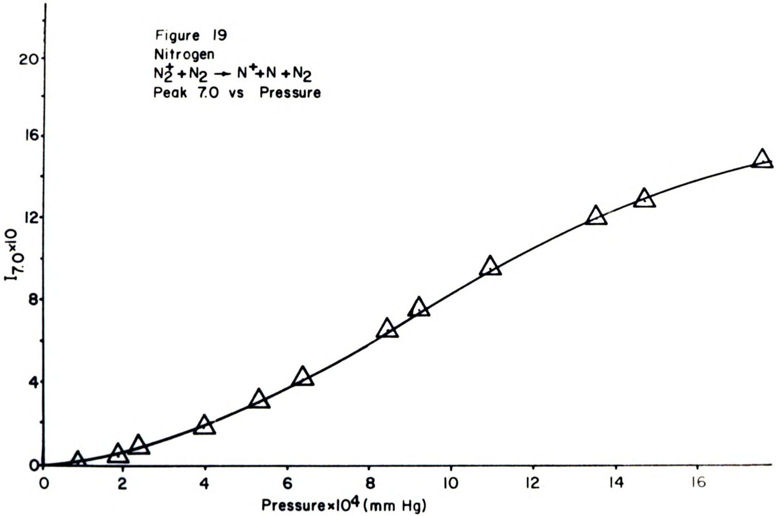

Figure 19
Nitrogen
$N_2^+ + N_2 \rightarrow N^+ + N + N_2$
Peak 7.0 vs Pressure

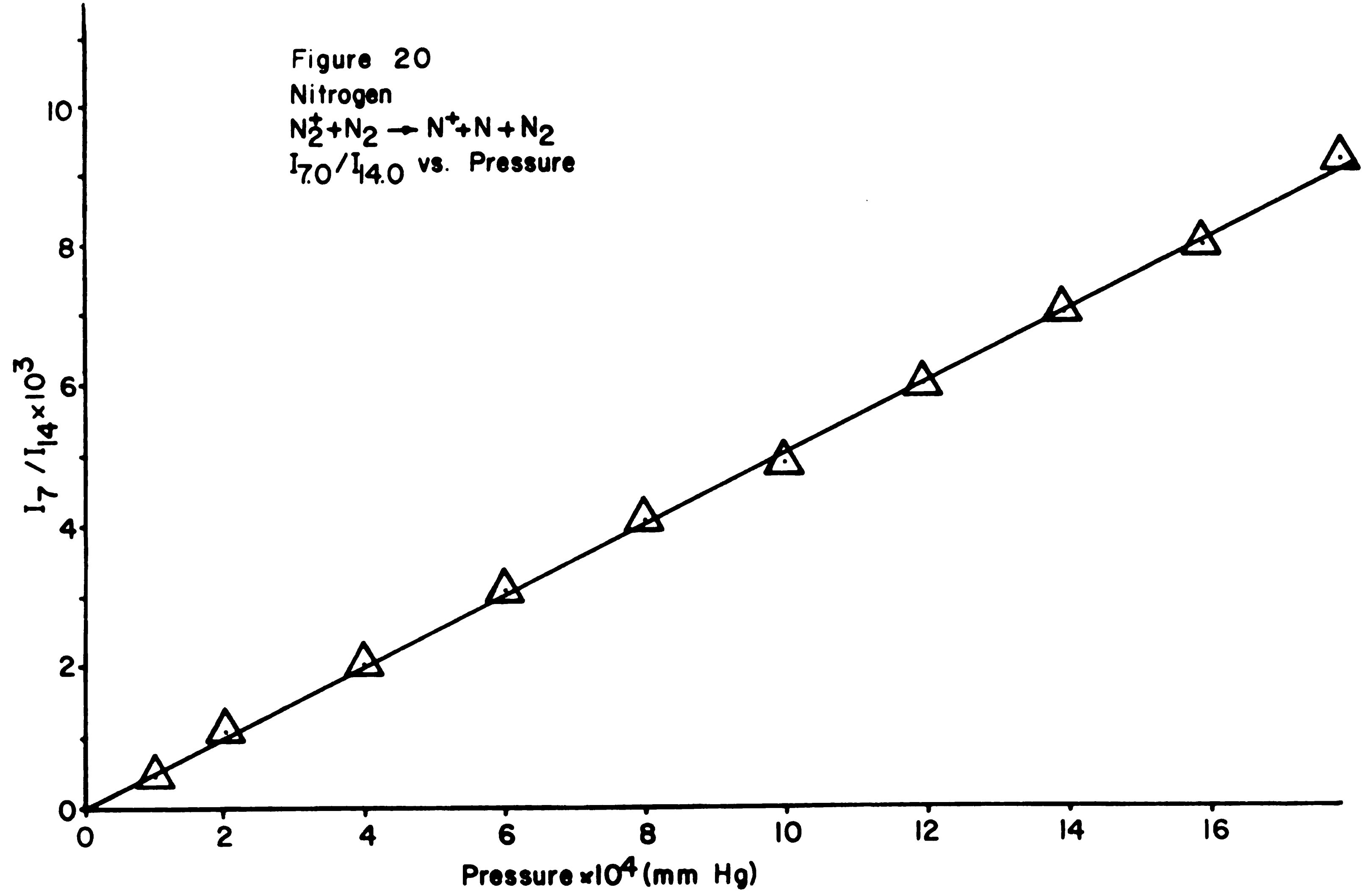

Figure 20
Nitrogen
$N_2^+ + N_2 \rightarrow N^+ + N + N_2$
$I_{7.0}/I_{14.0}$ vs. Pressure

E. Nitrous Oxide

The nitrous oxide system had been studied a number of times before the present work was begun, but only in a qualitative manner. In these earlier studies, the pressure in the collision volume was not measured directly, nor was the pressure gauge calibrated. Metastable contributions were reported by Begun and Landau (29), (30), with a spectrometer without repeller electrodes, but were denied by Friedman and Irsa (31). No cross sections were reported.

Although metastable transitions are not common in triatomic molecules, they have been reported in carbon dioxide (75) and in H_2S (76).

A recent paper by Newton and Sciamanna (77) confirms the existence of the metastable transition

(42) $N_2O^+ \longrightarrow NO^+ + N$

and measures the (unimolecular) half-life to be less than 0.2×10^{-6} sec. Since the residence time in the source for an ion of m/q 44 is about 4.6×10^{-7} sec at 15 volts repelling potential in our spectrometer, one might expect to observe some metastable transitions. However, a single rate constant does not indicate what portion of the ions will decompose at this rate. Newton and Sciamanna also neglected to report the electron energy used in their study. They could not measure cross sections for the collision-induced reaction because the pressure in their analyzer was not known.

In the present work, no metastable contribution to the peak at 20.45 was observed (Figure 23), but this should not be considered a refutation of the work of Newton and Sciamanna, or of Begun and Landau, since their experimental conditions may have been much different from those in the present work.

Since the nitrous oxide system was studied with the gas inlet exclusively, no measurements of total collision cross sections are possible, although the intensity of the NO^+ ion as a function of pressure is presented in Figure 21. The slope of Figure 23 yields a value of 1.24×10^{-16} cm^2 for the reaction

$$N_2O^+ + N_2O \longrightarrow NO^+ + N + N_2O \tag{43}$$

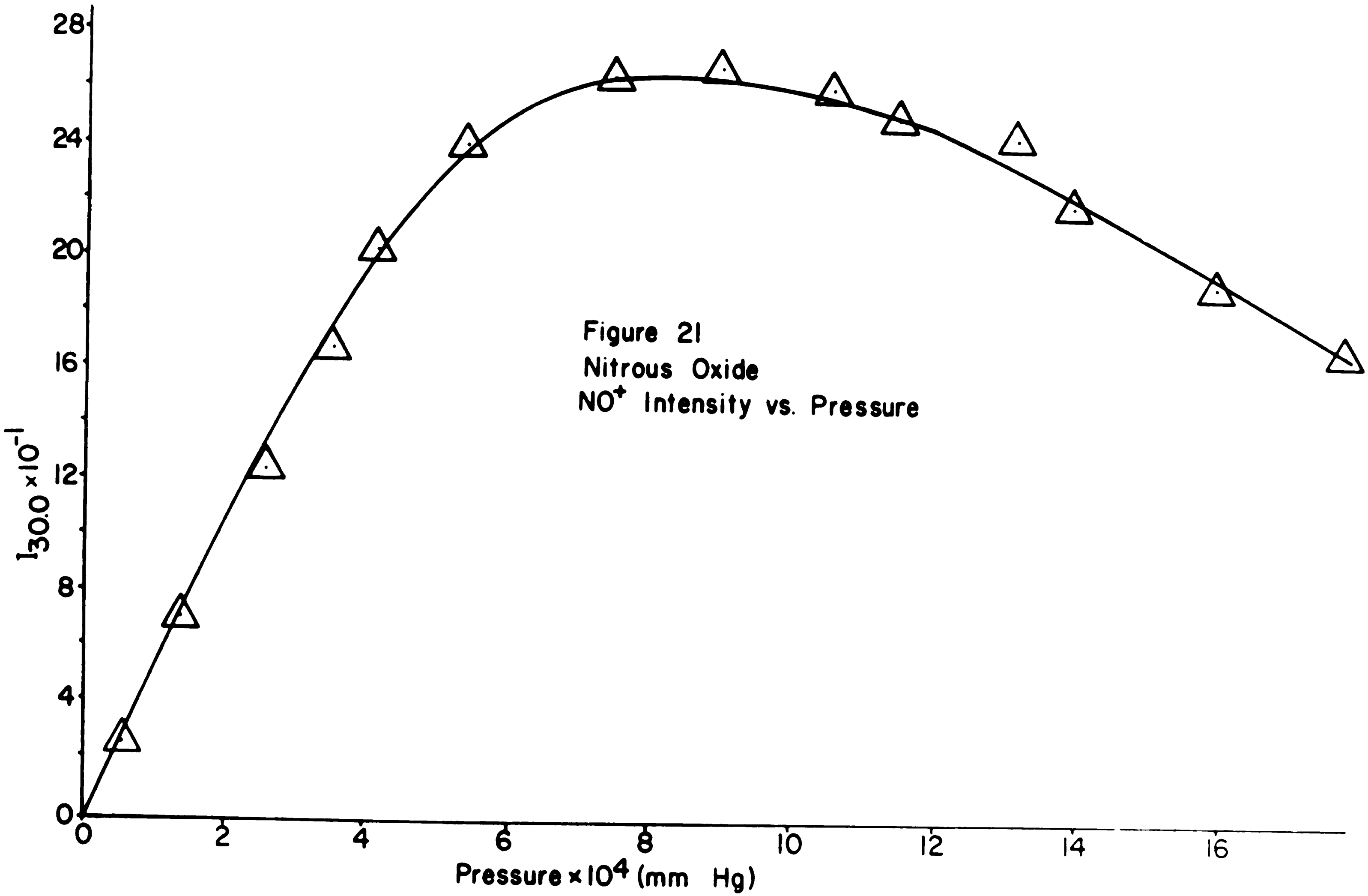

Figure 21
Nitrous Oxide
NO^+ Intensity vs. Pressure

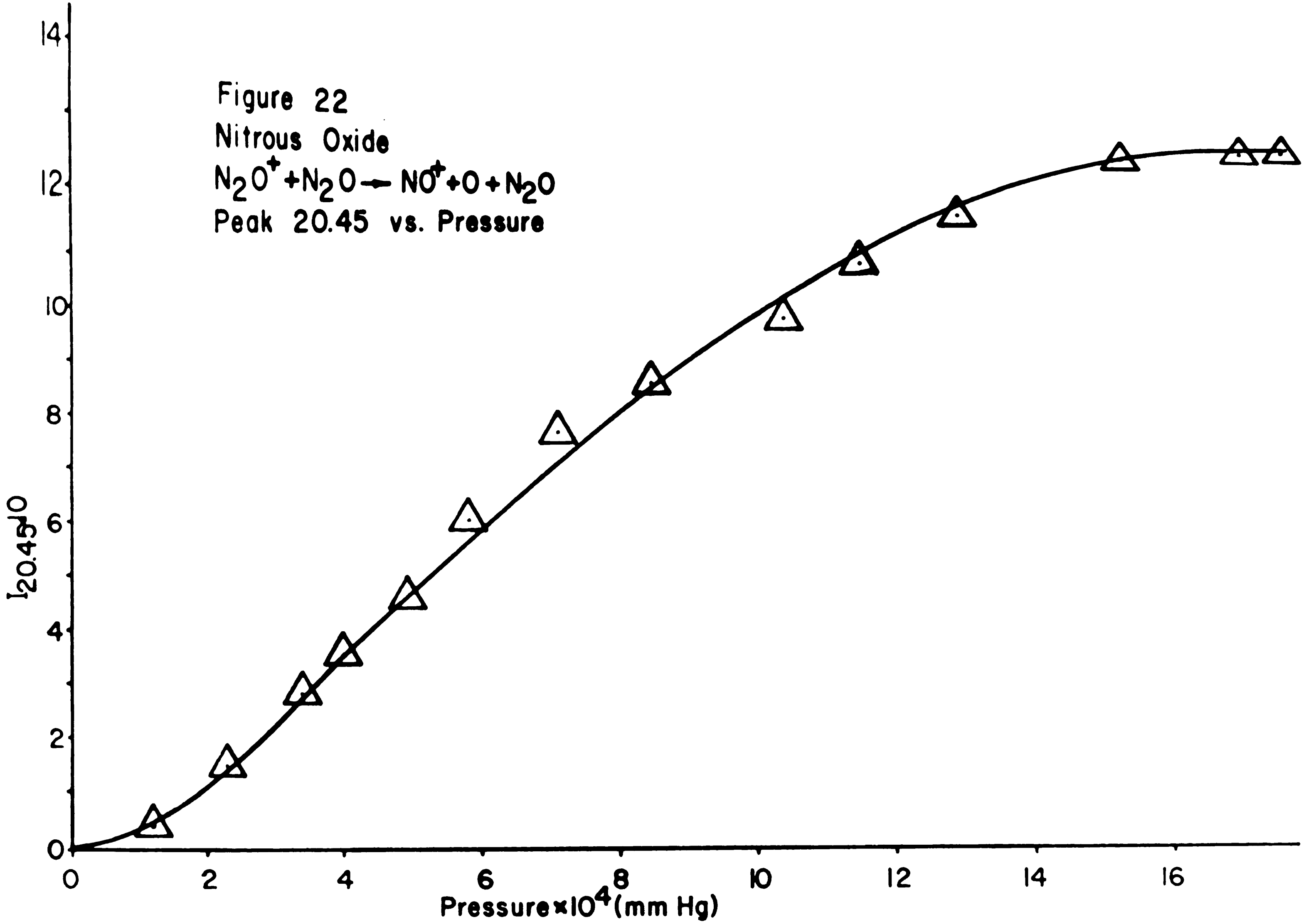

Figure 22
Nitrous Oxide
$N_2O^+ + N_2O \rightarrow NO^+ + O + N_2O$
Peak 20.45 vs. Pressure

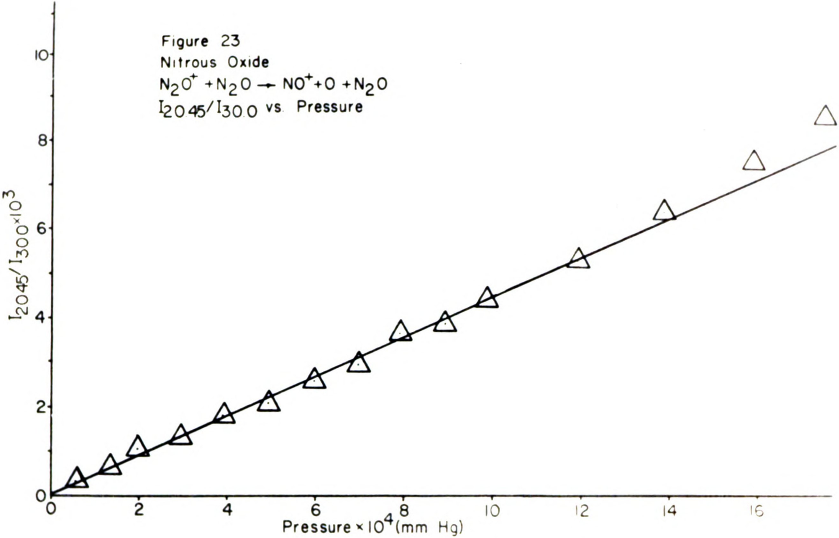

Figure 23
Nitrous Oxide
$N_2O^+ + N_2O \rightarrow NO^+ + O + N_2O$
$I_{20.45}/I_{30.0}$ vs. Pressure

VI. CONCLUSIONS AND SUGGESTIONS FOR FURTHER WORK

The primary advantage of the technique developed in this thesis is that quantitative measurements of the cross sections of collision-induced phenomena may be made without a specially built mass spectrometer. The required modifications to an analytical instrument are slight and do not preclude analytical use of the instrument. The spectrometer used in the experimental part of the present work was concurrently used for the analytical mass spectrometer requirements of the rest of the chemistry department. Such practical considerations, while not of scientific moment, often contribute strongly to the interest in a given field. It is hoped that many scientists with access to a Dempster-type analytical spectrometer will be encouraged to undertake measurements of this kind, knowing that such a project need not be expensive or elaborate.

A possibly useful bonus to the present method was discovered as the mass spectral data were being reduced. If the Aston band intensity is divided by the intensity of an ion other than the product ion, the resultant ratio will not, in general, be a linear function of pressure. This behavior could be useful in the identification of the origin of an Aston band. If one happened to choose a "wrong" ion that had the same total collision cross section as the product ion, the result would, however, be a straight line.

An important disadvantage to the technique of studying Aston bands in a Dempster spectrometer is that, because the source and the analyzer are both in the magnetic field, it is difficult to pump them separately. This means that one cannot study the collision of the ions of one gas on the molecules of another. It has occurred to the author that this difficulty could be circumvented by measuring the bands in a series of mixtures of the two gases and extrapolating to the pure gas. Such a procedure would be very time consuming.

The experimental cross sections reported in the present work should not be considered as significant contributions to the literature of collision-induced dissociations, but only as examples of the reactions which may easily be studied using the method developed in the theoretical section. Since the technique of studying collision-induced Aston bands in a Dempster spectrometer is established, it is hoped that these bands will be thoroughly reinvestigated, as a function of both electron energy and ion energy, in order to bring to light more of the details of the dissociation process. It is felt that the collision-induced band in nitrogen would be particularly fertile, since it has not previously been observed and nothing is known about the mechanism of its formation. An explanation should be found for the unusually low value for its cross section.

Additional theoretical work should be carried out to better define the length of the effective collision volume, both for collision-induced processes and for metastable transitions. The rudimentary calculations carried out in Appendix 2 are obviously inadequate, but it is expected that the recent work of Coggeshall (52) and Newton (78) will be extended to give a realistic estimate of the distance an ion can travel into the analyzer before dissociating and still be collected. It is anticipated that such a realistic estimate will require inclusion of the effect of the kinetic energy released on dissociation. In the absence of a complete theoretical treatment of the size and shape of the collision volume, the dependence of ℓ_4 on the radii of parent and daughter ions could be determined by a careful comparison of data obtained with a Dempster instrument with the results of measurements from a sector-field spectrometer having a well-defined collision chamber.

Newton (78) has shown that peak shapes of metastable transitions can only be explained by assuming that kinetic energy is released in the reaction. Presumably, these kinetic energy effects are also present in collision-induced dissociations, and, in addition, there is the probability that kinetic energy is transferred to the target ion. Since the mass spectrometer is essentially a momentum selector, these kinetic energy effects tend to widen the ion beam, and some ions are therefore lost by collision with slits. Of course, the number of ions lost is dependent on the size of the kinetic energy effects and the selectivity of the spectrometer. For this reason, very different cross section measurements may be obtained with different instruments. At the present time, neither the kinetic energy released by the reaction, nor that transferred to the target ion, is known, so that the effects may not be taken into account when absolute cross sections are compared. Fortunately, absolute cross sections are seldom of importance to the chemist. He is usually more interested in how the cross section varies with ion accelerating energy and with electron energy than in its absolute value. Therefore, although the Dempster spectrometer method shares the problem of the unknown kinetic energy effect with the sector-field method, it should not be a bar to its use.

VII. APPENDIX 1

The following pages present the results of the calibration experiments as described in the Experimental section. The calibrations of the ion gauge for argon, carbon monoxide, and nitrogen were performed with the cold trap cooled with liquid nitrogen. Since carbon dioxide and nitrous oxide condense at liquid nitrogen temperature, the trap was cooled in an acetone-dry ice bath for those runs.

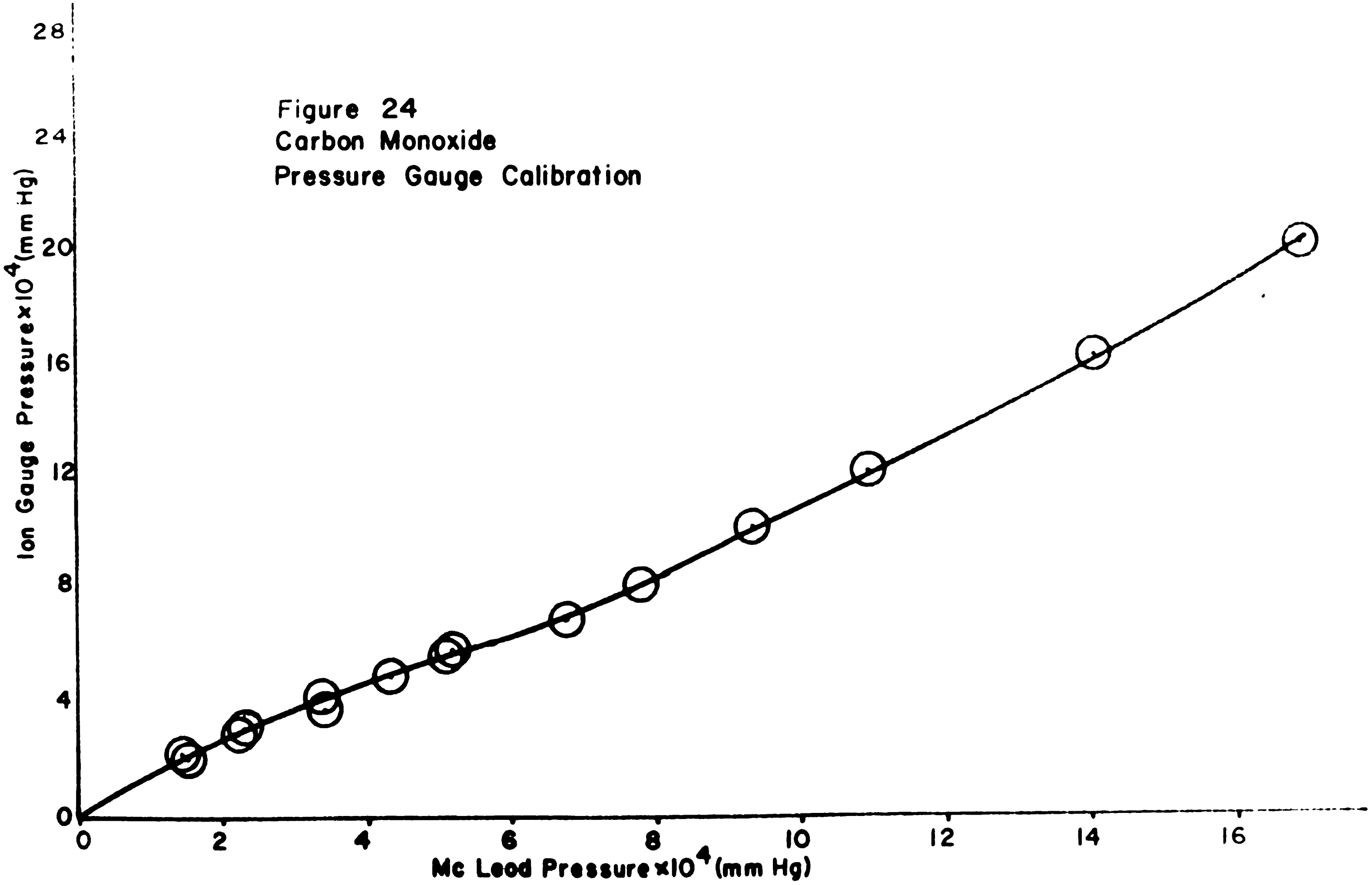

Figure 24
Carbon Monoxide
Pressure Gauge Calibration

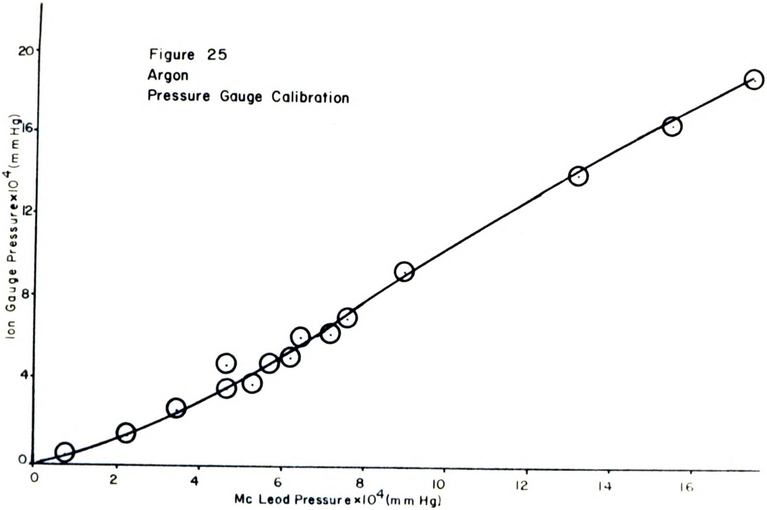

Figure 25
Argon
Pressure Gauge Calibration

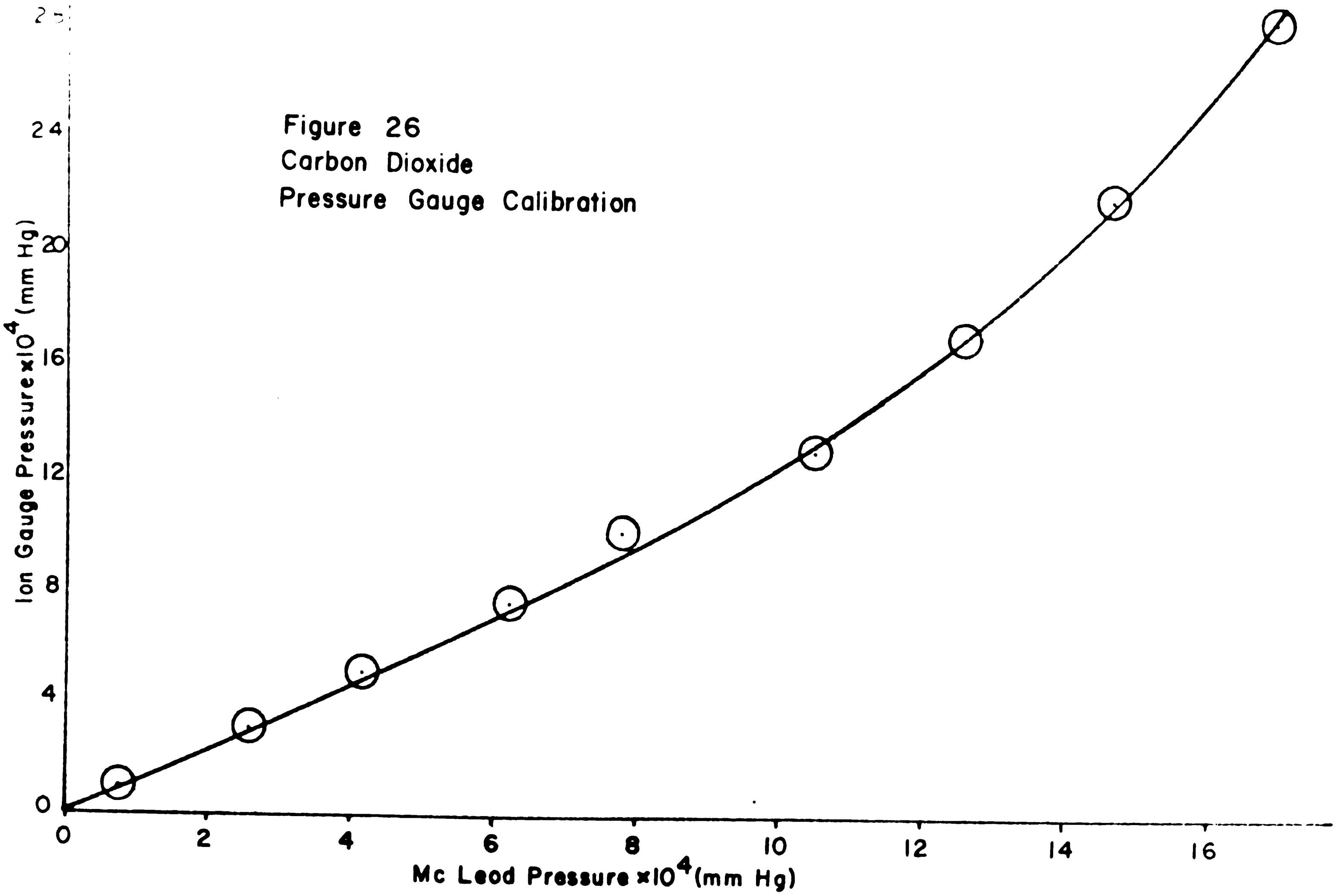

Figure 26
Carbon Dioxide
Pressure Gauge Calibration

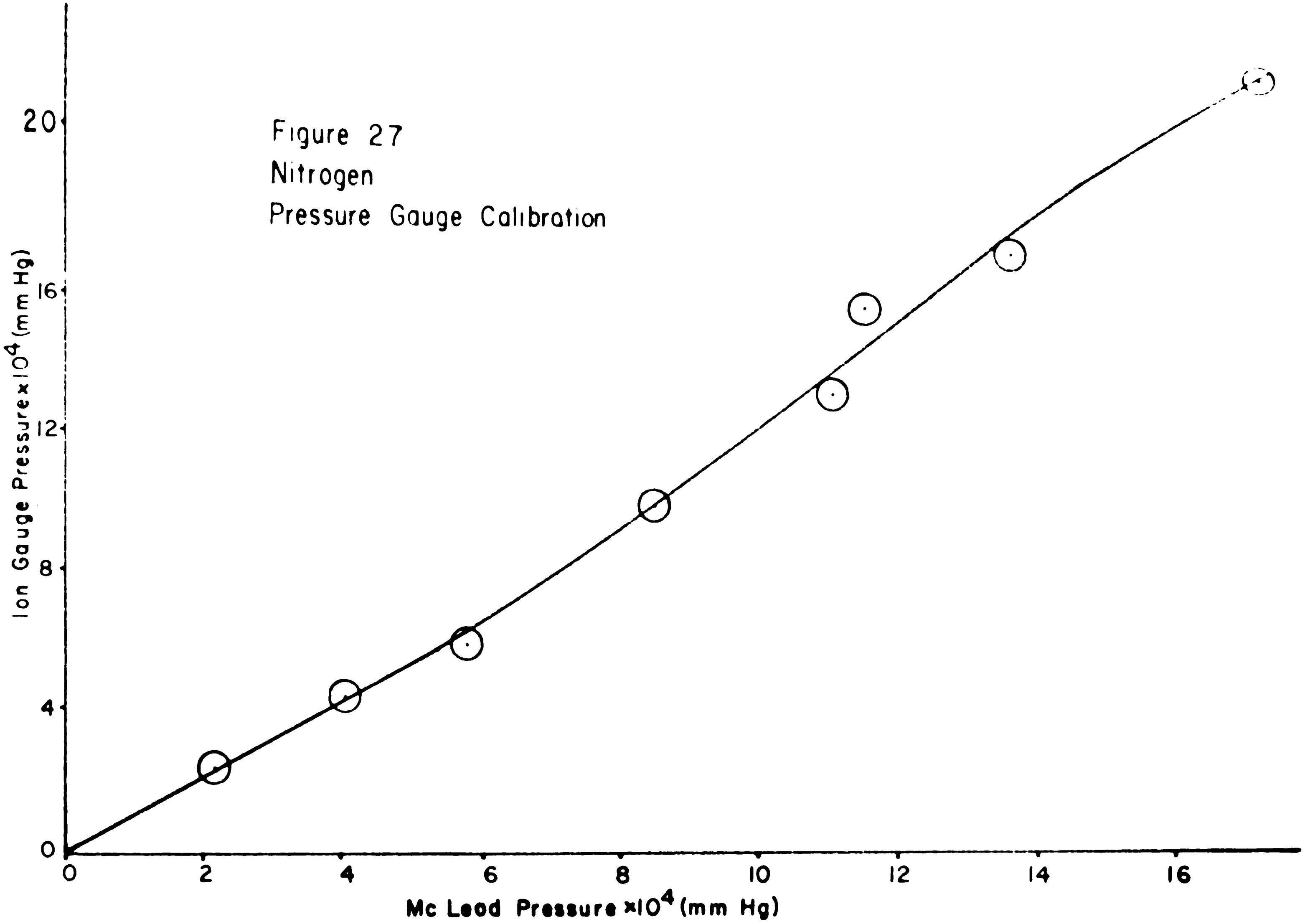

Figure 27
Nitrogen
Pressure Gauge Calibration

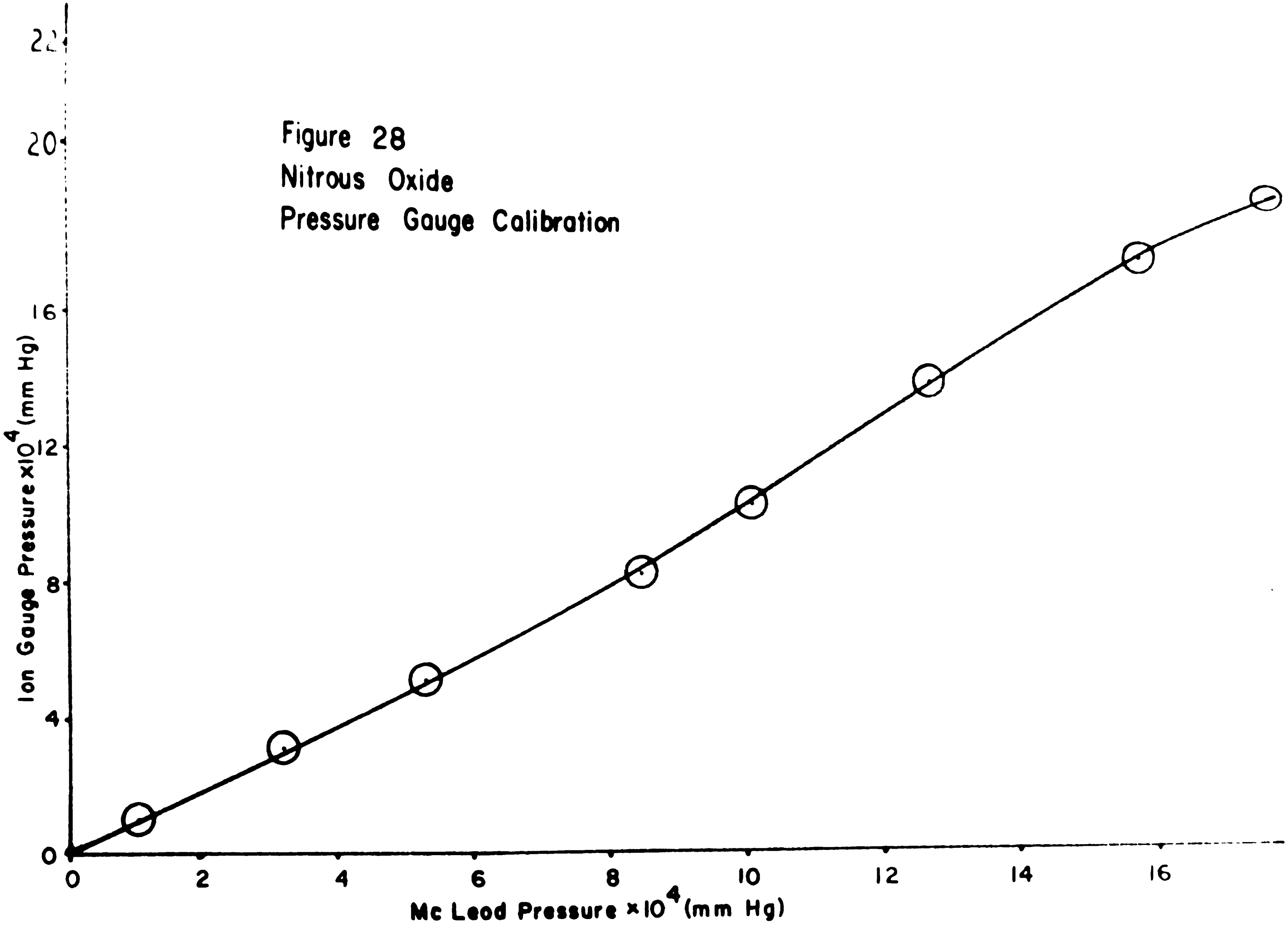

Figure 28
Nitrous Oxide
Pressure Gauge Calibration

VIII. APPENDIX 2

Coggeshall (52) has analyzed the path of a metastable ion in a Dempster mass spectrometer, for the purpose of explaining the peak shapes observed for metastable transitions. Although his analysis did not include kinetic energy effects, and he therefore did not obtain realistic peak shapes, his approach may lead to a first approximation to the length ℓ_4 of the effective collision volume for collision-induced reactions.

Figure 29 pictures the path of an ion in the analyzer of a Dempster spectrometer. The ion enters through a slit of width 2ϵ at the top of the figure. After travelling a distance in the analyzer, the ion may collide with a molecule and dissociate. When the ion dissociates, its radius changes from the initial value, R_1, to the radius R_2 characteristic of the product ion. The center of the circle described by the initial ion is constrained to the line between the entrance and exit slits by the fact that the ions enter perpendicular to this line. It may be seen that the ion path which leads to the maximum distance of travel before dissociation is one in which the ions pass very near the inside edges of the entrance and exit slits. This is the path illustrated in Figure 29.

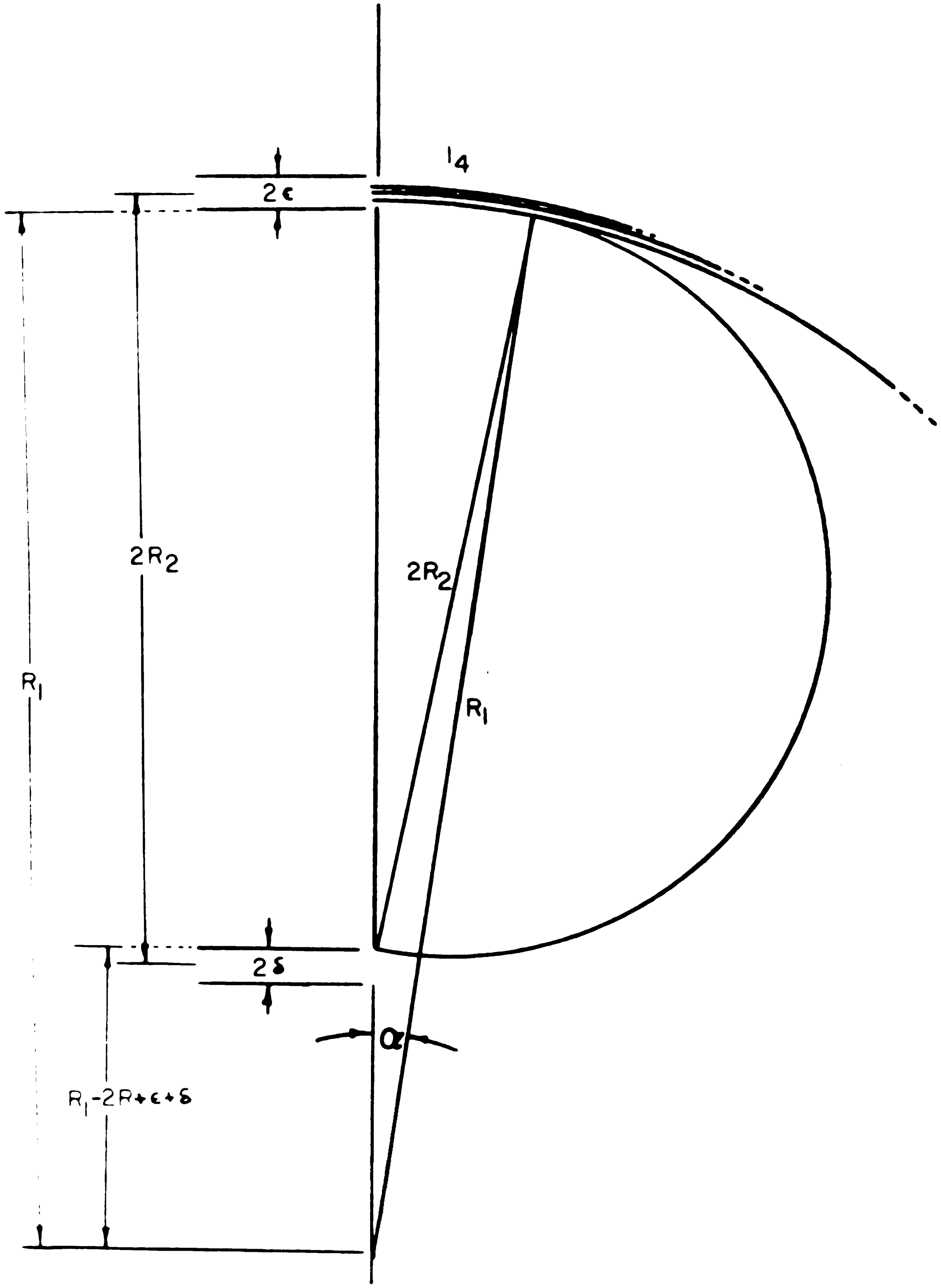

Figure 29. Geometric estimation of l_4.

The distance ℓ_4 may be obtained from a simple trigonometric argument. Consider the triangle formed by the center of the circle described by the initial ion, the exit slit, and the point where the ion dissociates. Applying the law of cosines to this triangle, the angle α is found to be

$$(1)\ \alpha = \cos^{-1}\left[\frac{2R_1^2 - 4R_1R_2 + 2R_1\epsilon + 2R_1\delta - 4R_2\epsilon - 4R_2\delta + \epsilon^2 + \delta^2 + 2\epsilon\delta}{2R_1^2 - 4R_1R_2 + 2R_1\epsilon + 2R_1\delta}\right]$$

The terms ϵ^2, δ^2, and $2\epsilon\delta$ will be much smaller than any others, and may be neglected. Then

$$(2)\ \alpha = \cos^{-1}\left[1 - \frac{2R_2\epsilon + 2R_2\delta}{R_1^2 - 2R_1R_2 + R_1\epsilon + R_1\delta}\right]$$

Now consider the triangle formed by the center of the circle of the initial ion, the entrance slit, and the dissociation point. Application of the law of cosines to this triangle yields

$$(3)\quad \ell_4 = \left[\frac{4R_1R_2(\epsilon + \delta)}{R_1 - 2R_2 + \epsilon + \delta}\right]^{\frac{1}{2}}$$

It is convenient to measure all of the distances as multiples of the analyzer radius R_2 (i.e. $R_2 = 1$). Neglecting ϵ and δ compared to R_1 and R_2,

$$(4)\quad \ell_4 = \left[\frac{4R_1(\epsilon + \delta)}{R_1 - 2}\right]^{\frac{1}{2}}$$

The analysis above was based on $R_1 > 2R_2$. For $R_1 < 2R_2$, the result is

$$(5) \qquad \ell_4 = \left[\frac{4R_1(\epsilon + \delta)}{2 - R_1}\right]^{\frac{1}{2}}$$

A singularity occurs when $R_1 = 2R_2$. In this case, the end of the effective collision volume is determined by the collision of the product ions with the wall of the analyzer.

It is of interest to see what the equations (4) and (5) predict for the length of the effective collision volume for the reactions studied in the present work. These results are tabulated in Table 2. The reaction $N_2^+ \longrightarrow N^+ + N$ is an example of the singular case, and the calculated ℓ_4 is determined by collision of the product ions with the wall of the analyzer. In the instrument used here, as in Coggeshall's instrument (52), this occurs when the ions have traversed an arc of 17°, or 3.77 cm.

TABLE 2

Theoretical ℓ_4 for Several Reactions

Reaction	ℓ_4 (cm)
$CO_2^+ + M \longrightarrow C^+ + O^+ + O + M$	0.522
$CO^+ + M \longrightarrow C^+ + O + M$	1.23
$Ar^{++} + M \longrightarrow Ar^+ + M^+$	0.271
$N_2^+ + M \longrightarrow N^+ + N + M$	3.77
$N_2O^+ + M \longrightarrow NO^+ + N + M$	0.782

The approximate nature of the above analysis should be emphasized. We have estimated the maximum distance that a reactant ion could penetrate the analyzer. In all cases except $R_1 = 2R_2$, this maximum penetration is achieved by an ion which passes very near the slits, and the collision volume for an average ion would be much smaller. For instance, if the collision volume is triangular, the average length ℓ_4 would be only half of the value calculated above. An analysis of the shape of the collision volume would be very difficult and would probably require computer calculation.

A second criticism of the analysis above is that the kinetic energy released in the dissociation was not considered. A semi-empirical study of metastable peak shapes by Newton (78) has shown that this parameter must be included in such an analysis. It would be expected to be of even greater importance in collision-induced reactions, since kinetic energy may be transferred to the target molecule.

Until the trajectories of ions undergoing reaction in a spectrometer are better understood, it is felt that the method of calibration employed in the present work is the best approximation.

IX. REFERENCES

1. F. W. Aston, Proc. Cambridge Phil. Soc., 19, 317 (1920).

2. F. W. Aston, Mass Spectra and Isotopes, 2nd ed. New York: Longmans, Green, and Co., 1941.

3. K. T. Bainbridge and E. B. Jordan, Phys. Rev., 51, 595 (1937).

4. J. Mattauch and H. Lichtblau, Phys. Zeit., 40, 16 (1939).

5. H. D. Smyth, Phys. Rev., 25, 452 (1925).

6. H. D. Smyth, Rev. Mod. Phys., 3, 347 (1931).

7. A. J. Dempster, Phys. Rev., 53, 64 (1938).

8. J. A. Hipple and E. U. Condon, Phys. Rev., 68, 54 (1945).

9. J. A. Hipple, R. E. Fox, and E. U. Condon, Phys. Rev., 69, 347 (1946).

10. J. A. Hipple, Phys. Rev., 71, 594 (1947).

11. O. Eisenhut, R. Conrad, Zeit. Electrochem., 36, 654 (1930).

12. W. Schutze, Wiss. Veroffentl. Siemens-Werken., 16, 89 (1937).

13. H. Ewald and A. Henglein, Z. Naturforsch., 6a, 463 (1951).

14. A. Henglein, Z. Naturforsch., 7a, 165 (1952).

15. G. F. Wells and C. E. Melton, Rev. Sci. Inst., 28, 1065 (1957).

16. C. E. Melton and G. F. Wells, J. Chem. Phys., 27, 1132 (1957).

17. C. E. Melton, M. M. Bretscher, and R. Baldock, J. Chem. Phys., 26, 1302 (1957).

18. C. E. Melton and H. M. Rosenstock, J. Chem. Phys., 26, 568 (1957).

19. H. M. Rosenstock and C. E. Melton, J. Chem. Phys., 26, 314 (1957).

20. C. E. Melton and G. A. Ropp, J. Chem. Phys., 29, 400 (1958).

21. L. Kerwin, Rev. Sci.,Inst., 21, 96 (1950).

22. J. D. Carette and L. Kerwin, Can. J. Phys., 39, 1300 (1961).

23. W. McGowan and L. Kerwin, Can. J. Phys., 38, 642 (1960).

24. W. McGowan and L. Kerwin, Can. J. Phys., 41, 316 (1963).

25. N. M. Tunitskii, P. M. Smirnova, and M. V. Tikhomirov, Doklady Akad. Nauk. SSSR, 101, 1083 (1955).

26. A. P. Irsa and L. Friedman, J. Chem. Phys., 34, 330 (1960).

27. M. V. Tikhomirov, V. M. Kolotyrkin, and N. M. Tunitskii, Doklady Akad. Nauk. SSSR, 101, 903 (1955).

28. V. M. Kolotyrkin, M. V. Tikhomirov, N. M. Tunitskii, Doklady Akad. Nauk. SSSR, 92, 1193 (1953).

29. G. M. Begun and L. Landau, J. Chem. Phys., 35, 547 (1961).

30. G. M. Begun and L. Landau, J. Chem. Phys., 36, 1083 (1961).

31. L. Friedman and A. P. Irsa, J. Chem. Phys., 36, 1082 (1961).

32. W. A. Chupka and K. M. A. Refaey, Argonne National Laboratory Informal Report PHY-1966A, May 1966.

33. E. Lindholm, Proc. Phys. Soc., 66A, 1068 (1953).

34. E. Lindholm, Arkiv Fys., 8, 433 (1954).

35. E. Lindholm and H. von Koch, Arkiv Fys., 19, 123 (1961).

36. N. V. Fedorenko, Zhur. Tekh. Fiz., 24, 769 (1954).

37. F. M. Rourke, J. C. Sheffield, W. D. Davis, and F. A. White, J. Chem. Phys., 31, 193 (1959).

38. J.-C. Abbe and J.-P. Adloff, C. R. Acad. Sc. Paris., 258, 3003 (1964)

39. J.-C. Abbe and J.-P. Adloff, Physics Letters, 11, 28 (1964).

40. J.-C. Abbe and J.-P. Adloff, Bull. Soc. Chim. France, 1964, 1212.

41. M. Inghram and R. Gomer, Z. Naturforsch., 10a, 863 (1955).

42. J. B. Hasted, Proc. Conf. Ioniz. Phen. Gases Munich. 1961. p. 11.

43. J. B. Hasted, J. T. Scott, and A. Y. J. Chong, Proc. Conf. Ioniz. Phen. Gases Uppsala., 1959. p. 34.

44. H. B. Gilbody, J. B. Hasted, J. V. Ireland, A. R. Lee, E. W. Thomas, and A. S. Whiteman, Proc. Roy. Soc. (London), 274a, 40 (1963).

45. M. Islam, J. B. Hasted, H. B. Gilbody, and J. V. Ireland, Proc. Phys. Soc., 79, 1118 (1962).

46. J. B. Hasted and R. A. Smith, Proc. Roy. Soc. (London), 235a, 354 (1956).

47. J. B. Hasted in Bates, ed., Atomic and Molecular Processes, New York: Academic Press, 1965.

48. W. W. Hunt, R. E. Huffman, J. Saari, G. Wassel, J. F. Betts, E. H. Pauve, W. Wyess, and R. A. Flugge, Air Force Cambridge Research Laboratories Research Pro-Report AFCRL-63-708 (1963).

49. W. W. Hunt, R. E. Huffman, K. E. McGee, Rev. Sci. Inst., 35, 82 (1964).

50. R. E. Ferguson, K. E. McCulloh, and H. M. Rosenstock, J. Chem. Phys., 42, 100 (1965).

51. H. S. W. Massey and E. H. S. Burhop, Electronic and Ionic Impact Phenomena, Oxford: Clarendon Press, 1952, p. 2.

52. N. D. Coggeshall, J. Chem. Phys., 37, 2167 (1962).

53. V. Nikolaev, D. Dmitriev, L. Fateeva, and Y. Teplova, Zh. Eksperium. i Teor. Fiz., 40, 989 (1961).

54. S. Kuprianov, M. Tikhomirov, V. Potapov, and P. Karpova, Soviet Physics-JETP, 30, 569 (1956).

55. C. E. Melton in F. W. McLafferty, ed., Mass Spectrometry of Organic Ions, New York: Academic Press, 1963, Chapter 2.

56. M. Ackerman, J. Drowart, P. Goldfinger, and M. Jeunehomme, J. Chem. Phys., 26, 978 (1957).

57. W. Gaede, Ann. Phys., 46, 354 (1915).

58. H. Ishii and N. Nakayama, Trans. Natl. Vac. Sym. 8th 1961, 1, 519 (1962).

59. C. Meinke and G. Reich, Vacuum, 13, 579 (1963).

60. C. Meinke and G. Reich, Vacuum-Technik, 11, 86 (1962).

61. B. L. Schramm, M. J. van der Wiel, F. J. de Heer, and H. R. Moustafa, J. Chem. Phys., 44, 49 (1966).

62. E. W. Rothe, J. Vac. Sci. Tech., 1, 66 (1964).

63. American Petroleum Institute Project 44, Mass Spectral Data.

64. S. Kuprianov, Zh. Tekhn. Fiz., 34, 861 (1964).

65. F. Stuber, J. Chem. Phys., 42, 2639 (1965).

66. J. B. Hasted, Physics of Atomic Collisions, London: Butterworths, 1964.

67. J. Hornbeck and J. Molnar, Physical Review, 84, 621 (1951).

68. F. L. Mohler, National Bureau of Standards, Technical Note No. 243 (1964).

69. W. Cramer, J. Chem. Phys., 30, 641 (1959).

70. E. Weiner, G. Hertel, and W. Koski, J. Chem. Phys., 39, 3538 (1963).

71. J. Hasted, D. Phil., and R. Smith, Proc. Royal Soc. London, A235, 354 (1956).

72. I. Flaks and E. Solov'ev, Soviet Physics-Technical Physics, 3, 564 (1958).

73. V. Potapov, Zhur. Fiz. Khim., 34, 444 (1960).

74. D. Wobschall, J. Graham, and D. Malone, Physics Review, 131, 1567 (1963).

75. A. Newton and A. Sciamanna, J. Chem. Phys., 40, 718 (1964).

76. V. Dibeler and H. Rosenstock, J. Chem. Phys., 39, 3106 (1963).

77. A. Newton and A. Sciamanna, J. Chem. Phys., 44, 4327 (1966).

78. A. Newton, J. Chem. Phys., 44, 4015 (1966).